

# USING SIAM'S L<sup>A</sup>T<sub>E</sub>X MACROS\*

PAUL DUGGAN†

**Abstract.** Documentation is given for use of the SIAM L<sup>A</sup>T<sub>E</sub>X macros. These macros are now compatible with L<sup>A</sup>T<sub>E</sub>X2<sub>ε</sub>. Instructions and suggestions for compliance with SIAM style standards are also included. Familiarity with standard L<sup>A</sup>T<sub>E</sub>X commands is assumed.

**Key words.**

**AMS subject classifications.**

**1. Introduction.** This file is documentation for the SIAM L<sup>A</sup>T<sub>E</sub>X macros, and provides instruction for submission of your files.

To accommodate authors who electronically typeset their manuscripts, SIAM supports the use of L<sup>A</sup>T<sub>E</sub>X. To ensure quality typesetting according to SIAM style standards, SIAM provides a L<sup>A</sup>T<sub>E</sub>X macro style file. Using L<sup>A</sup>T<sub>E</sub>X to format a manuscript should simplify the editorial process and lessen the author's proofreading burden. However, it is still necessary to proofread the galley proofs with care.

Electronic files should not be submitted until the paper has been accepted, and then not until requested to do so by someone in the SIAM office. Once an article is slated for an issue, someone from the SIAM office will contact the author about any or all of the following: editorial and stylistic queries, supplying the source files (and any supplementary macros) for the properly formatted article, and handling figures.

When submitting electronic files (electronic submissions) (to [tex@siam.org](mailto:tex@siam.org)) include the journal, issue, and author's name in the subject line of the message. Authors are responsible for ensuring that the paper generated from the source files exactly matches the paper that was accepted for publication by the review editor. If it does not, information on how it differs should be indicated in the transmission of the file. When submitting a file, please be sure to include any additional macros (other than those provided by SIAM) that will be needed to run the paper.

SIAM uses MS-DOS-based computers for L<sup>A</sup>T<sub>E</sub>X processing. Therefore all filenames should be restricted to eight characters or less, plus a three character extension.

Once the files are corrected here at SIAM, we will mail the revised proofs to be read against the original edited hardcopy manuscript. We are not set up to shuttle back and forth varying electronic versions of each paper, so we must rely on hard copy of the galleys. The author's proofreading is an important but easily overlooked step. Even if SIAM were not to introduce a single editorial change into your manuscript, there would still be a need to check, because electronic transmission can introduce errors.

The distribution contains the following items: `siamltex.cls`, the main macro package based on `article.cls`; `siam10.clo`, for the ten-point size option; `subeqn.clo`, a style option for equation numbering (see §3 for an explanation); and `siam.bst`, the style file for use with BIB<sub>T</sub>E<sub>X</sub>. Also included are this file `docultex.tex` and a sample file `lexample.tex`. The sample file represents a standard application of the macros. The rest of this paper will highlight some keys to effective macro use,

---

\*This work was supported by the Society for Industrial and Applied Mathematics

†Society for Industrial and Applied Mathematics, Philadelphia, Pennsylvania. ([duggan@siam.org](mailto:duggan@siam.org)). Questions, comments, or corrections to this document may be directed to that email address.

as well as point out options and special cases, and describe SIAM style standards to which authors should conform.

**2. Headings.** The top matter of a journal paper falls into a standard format. It begins of course with the `\documentclass` command

```
\documentclass{siamltex}
```

Other class options can be included in the bracketed argument of the command, separated by commas.

Optional arguments include:

**final** Without this option, lines which extend past the margin will have black boxes next to them to help authors identify lines that they need to fix, by re-writing or inserting breaks. **final** turns these boxes off, so that very small margin breaks which are not noticeable will not cause boxes to be generated.

**oneeqnum** Normally `siamltex.cls` numbers equations, tables, figures, and theorem environments with a decimal number, composed of the section of the paper, a period, and the number of the enumerated object (example: 1.2). The sequence of numbering is also restarted with each new section, so that, for example, the last equation of section 3 may be 3.10, but the first equation of section 4 would be 4.1. Using **oneeqnum** numbers all equations consecutively throughout a paper with a single digit.

**onethmnum** Using **onethmnum** numbers all theorem-like environments consecutively throughout a paper with a single digit.

**onefignum** Using **onethmnum** numbers all figures consecutively throughout a paper with a single digit.

**onetabnum** Using **onethmnum** numbers all tables consecutively throughout a paper with a single digit.

The title and author parts are formatted using the `\title` and `\author` commands as described in Lamport [3]. The `\date` command is not used. `\maketitle` produces the actual output of the commands.

The addresses and support acknowledgments are put into the `\author` commands via `\thanks`. If support is overall for the authors, the support acknowledgment should be put in a `\thanks` command in the `\title`. Specific support should go following the addresses of the individual authors in the same `\thanks` command.

Sometimes authors have support or addresses in common which necessitates having multiple `\thanks` commands for each author. Unfortunately  $\LaTeX$  does not normally allow this, so a special procedure must be used. An example of this procedure follows. Grant information can also be run into both authors' footnotes.

```
\title{TITLE OF PAPER}
```

```
\author{A.~U. Thorone\footnotemark[2]\ \footnotemark[5]
\and A.~U. Thortwo\footnotemark[3]\ \footnotemark[5]
\and A.~U. Thorthree\footnotemark[4]}
```

```
\begin{document}
\maketitle
```

```
\renewcommand{\thefootnote}{\fnsymbol{footnote}}
```

```

\footnotetext[2]{Address of A.~U. Thorone}
\footnotetext[3]{Address of A.~U. Thortwo}
\footnotetext[4]{Address of A.~U. Thorthree}
\footnotetext[5]{Support in common for the first and second
authors.}

\renewcommand{\thefootnote}{\arabic{footnote}}

```

Notice that the footnote marks begin with [2] because the first mark (the asterisk) will be used in the title for date-received information by SIAM, even if not already used for support data. This is just one example; other situations follow a similar pattern.

Following the author and title is the abstract, key words listing, and AMS subject classification number(s), designated using the `{abstract}`, `{keywords}`, and `{AMS}` environments. If there is only one AMS number, the commands `\begin{AM}` and `\end{AM}` are used instead of `{AMS}`. This causes the heading to be in the singular. Authors are responsible for providing AMS numbers. They can be found in the Annual Index of Math Reviews, or through e-Math (telnet e-math.ams.com; login and password are both e-math).

Left and right running heads should be provided in the following way.

```

\pagestyle{myheadings}
\thispagestyle{plain}
\markboth{A.~U. THORONE AND A.~U. THORTWO}{SHORTER PAPER
TITLE}

```

**3. Equations and mathematics.** One advantage of L<sup>A</sup>T<sub>E</sub>X is that it can automatically number equations and refer to these equation numbers in text. While plain T<sub>E</sub>X's method of equation numbering (explicit numbering using `\leqno`) works in the SIAM macro, it is not preferred except in certain cases. SIAM style guidelines call for aligned equations in many circumstances, and L<sup>A</sup>T<sub>E</sub>X's `{eqnarray}` environment is not compatible with `\leqno` and L<sup>A</sup>T<sub>E</sub>X is not compatible with the plain T<sub>E</sub>X command `\eqalign` and `\leqalignno`. Since SIAM may have to alter or realign certain groups of equations, it is necessary to use the L<sup>A</sup>T<sub>E</sub>X system of automatic numbering.

Sometimes it is desirable to designate subequations of a larger equation number. The subequations are designated with (roman font) letters appended after the number. SIAM has supplemented its macros with the `subeqn.clo` option which defines the environment `{subequations}`.

```

\begin{subequations}\label{EKx}
\begin{equation}
y_k = B y_{k-1} + f, \quad k=1,2,3,\ldots
\end{equation}
for any initial vector $ y_0$. Then
\begin{equation}
y_k \rightarrow u \quad \text{\mbox{\quad iff\quad}} \quad \rho(B) < 1.
\end{equation}
\end{subequations}

```

All equations within the `{subequations}` environment will keep the same overall number, but the letter designation will increase.

Clear equation formatting using  $\TeX$  can be challenging. Aside from the regular  $\TeX$  documentation, authors will find Nicholas J. Higham’s book *Handbook of Writing for the Mathematical Sciences* [2] useful for guidelines and tips on formatting with  $\TeX$ . The book covers many other topics related to article writing as well.

Authors commonly make mistakes by using `<`, `>`, `\mid`, and `\parallel` as delimiters, instead of `\langle`, `\rangle`, `|`, and `\lvert`. The incorrect symbols have particular meanings distinct from the correct ones and should not be confused.

TABLE 3.1  
*Illustration of incorrect delimiter use.*

Wrong		Right	
<code>&lt;x, y&gt;</code>	<code>&lt; x, y &gt;</code>	<code>\langle x, y\rangle</code>	<code>\langle x, y\rangle</code>
<code>5 &lt; \mid A \mid</code>	<code>5 &lt;  A  </code>	<code>5 &lt;  A </code>	<code>5 &lt;  A </code>
<code>6x = \parallel x</code>			
<code>- 1\parallel_{i}</code>	<code>6x =    x - 1   _i</code>	<code>6x = \lvert x - 1 \lvert_{i}</code>	<code>6x =   x - 1  _i</code>

Another common author error is to put large (and even medium sized) matrices in-line with the text, rather than displaying them. This creates unattractive line spacing problems, and should be assiduously avoided. Text-sized matrices (like  $\begin{pmatrix} a & b \\ b & c \end{pmatrix}$ ) might be used but anything much more complex than the example cited will not be easy to read and should be displayed.

More information on the formatting of equations and aligned equations is found in Lamport [3]. Authors bear primary responsibility for formatting their equations within margins and in an aesthetically pleasing and informative manner.

The SIAM macros include additional roman math words, or “log-like” functions, to those provided in standard  $\TeX$ . The following commands are added: `\const`, `\diag`, `\grad`, `\Range`, `\rank`, and `\supp`. These commands produce the same word as the command name in math mode, in upright type.

**4. Special fonts.** SIAM supports the use of the AMS- $\TeX$  fonts (version 2.0 and later). The package `amsfonts` can be included with the command `\usepackage{amsfonts}`. This package is part of the AMS- $\TeX$  distribution, available from the AMS or from the Comprehensive TeX Archive Network (anonymous ftp to ftp.shsu.edu). The blackboard bold font in this font package can be used for designating number sets. This is preferable to other methods of combining letters (such as  $\mathbb{I}$  and  $\mathbb{R}$  for the real numbers) to produce pseudo-bold letters but this is tolerable as well. Typographically speaking, number sets may simply be designated using regular bold letters; the blackboard bold typeface was designed to fulfil a desire to simulate the limitations of a chalk board in printed type.

**4.1. Punctuation.** All standard punctuation and all numerals should be set in roman type (upright) even within italic text. The only exceptions are periods and commas. They may be set to match the surrounding text.

References to sections should use the symbol  $\S$ , generated by `\S`. (If the reference begins a sentence, the term “Section” should be spelled out in full.) Authors should not redefine `\S`, say, to be a calligraphic  $\mathcal{S}$ , because `\S` must be reserved for use as the section symbol.

Authors sometimes confuse the use of various types of dashes. Hyphens (-, -) are used for some compound words (many such words should have no hyphen but must be run together, like “nonzero,” or split apart, like “well defined”). Minus signs (\$-\$, -) should be used in math to represent subtraction or negative numbers. En dashes (--, -) are used for ranges (like 3–5, June–August), or for joined names (like Runge–Kutta). Em dashes (---, —) are used to set off a clause—such as this one—from the rest of the sentence.

**4.2. Text formatting.** SIAM style preferences do not make regular use of the `{enumerate}` and `{itemize}` environments. Instead, `siamltex.cls` includes definitions of two alternate list environments, `{renumerate}` and `{romannum}`. Unlike the standard itemized lists, these environments do not indent the secondary lines of text. The labels, whether defaults or the optional user-defined, are always aligned flush right.

The `{renumerate}` environment consecutively numbers each item with an arabic numeral followed by a period. This number is always upright, even in slanted environments. (For those wondering at the unusual naming of this environment, it comes from Seroul and Levy’s [4] definition of a similar macro for plain T<sub>E</sub>X: `\meti` which is `\item` spelled backwards. Thus `{renumerate}` a portion of `{enumerate}` spelled backwards.)

The `{romannum}` environment consecutively numbers each item with a lower-case roman numeral enclosed in parentheses. This number will always be upright within slanted environments (as in theorems).

**5. Theorems and Lemmas.** Theorems, lemmas, corollaries, definitions, and propositions are covered in the SIAM macros by the theorem-environments `{theorem}`, `{lemma}`, `{corollary}`, `{definition}` and `{proposition}`. These are all numbered in the same sequence and produce labels in small caps with an italic body. Other environments may be specified by the `\newtheorem` command. SIAM’s style is for Remarks and Examples to appear with italic labels and an upright roman body.

```
\begin{theorem}
Sample theorem included for illustration.
Numbers and parentheses, like equation $(3.2)$, should be set
in roman type. Note that words (as opposed to ‘‘log-like’’
functions) in displayed equations, such as
$$ x^2 = Y^2 \sin z^2 \mbox{ for all } x $$
will appear in italic type in a theorem, though normally
they should appear in roman.\end{theorem}
```

This sample produces Theorem 4.1 below.

**THEOREM 5.1.** *Sample theorem included for illustration. Numbers and parentheses, like equation (3.2), should be set in roman type. Note that words (as opposed to “log-like” functions) in displayed equations, such as*

$$x^2 = Y^2 \sin z^2 \text{ for all } x$$

*will appear in italic type in a theorem, though normally they should appear in roman.*

Proofs are handled with the `\begin{proof}` `\end{proof}` environment. A “QED” box □ is created automatically by `\end{proof}`, but this should be preceded with a `\qquad`.

Named proofs, if used, must be done independently by the authors. SIAM style specifies that proofs which end with displayed equations should have the QED box two ems (`\qqquad`) from the end of the equation on line with it horizontally. Below is an example of how this can be done:

```
{\em Proof}. Proof of the previous theorem
```

```
.
.
.
```

```
thus,
```

```
$$
```

```
a^2 + b^2 = c^2 \qqquad\endproof
```

```
$$
```

**6. Figures and tables.** Figures and tables sometimes require special consideration. Tables in SIAM style are need to be set in eight point size by using the `\footnotesize` command inside the `\begin{table}` environment. Also, they should be designed so that they do not extend beyond the text margins.

SIAM style requires that no figures or tables appear in the references section of the paper.  $\LaTeX$  is notorious for making figure placement difficult, so it is important to pay particular attention to figure placement near the references in the text. All figures and tables should be referred to in the text.

SIAM supports the use of `epsfig` for including POSTSCRIPT figures. All POSTSCRIPT figures should be sent in separate files. See the `epsfig` documentation (available via anonymous ftp from CTAN: ftp.shsu.edu) for more details on the use of this style option. It is a good idea to submit high-quality hardcopy of all POSTSCRIPT figures just in case there is difficulty in the reproduction of the figure. Figures produced by other non- $\TeX$  methods should be included as high-quality hardcopy when the manuscript is submitted.

POSTSCRIPT figures that are sent should be generated with sufficient line thickness. Some past figures authors have sent had their line widths become very faint when SIAM set the papers using a high-quality 1200dpi printer.

Hardcopy for non-POSTSCRIPT figures should be included in the submission of the hardcopy of the manuscript. Space should be left in the `{figure}` command for the hardcopy to be inserted in production.

**7. Bibliography and Bib $\TeX$ .** If using Bib $\TeX$ , authors need not submit the `.bib` file for their papers. Merely submit the completed `.bbl` file, having used `siam.bst` as their bibliographic style file. `siam.bst` only works with Bib $\TeX$  version 99i and later. The use of Bib $\TeX$  and the preparation of a `.bib` file is described in greater detail in [3].

If not using Bib $\TeX$ , SIAM bibliographic references follow the format of the following examples:

```
\bibitem{Ri} {\sc W. Riter},
{\em Title of a paper appearing in a book}, in The Book
Title, E.~D. One, E.~D. Two, and A.~N. Othereditor, eds.,
Publisher, Location, 1992, pp.~000--000.
```

```
\bibitem{AuTh1} {\sc A.~U. Thorone}, {\em Title of paper
```

with lower case letters}, SIAM J. Abbrev. Correctly, 2 (1992), pp.~000--000.

```
\bibitem{A1A2} {\sc A.~U. Thorone and A.~U. Thortwo}, {\em
Title of paper appearing in book}, in Book Title: With All
Initial Caps, Publisher, Location, 1992.
```

```
\bibitem{A1A22} \sameauthor, % generates the 3 em rule
{\em Title of Book{\rm :} Note Initial Caps and {\rm ROMAN
TYPE} for Punctuation and Acronyms}, Publisher,
Location, pp.~000--000, 1992.
```

```
\bibitem{AuTh3} {\sc A.~U. Thorthree}, {\em Title of paper
that's not published yet}, SIAM. J. Abbrev. Correctly, to appear.
```

Other types of references fall into the same general pattern. See the sample file or any SIAM journal for other examples. Authors must correctly format their bibliography to be considered as having used the macros correctly. An incorrectly formatted bibliography is not only time-consuming for SIAM to process but it is possible that errors may be introduced into it by keyboarders/copy editors.

As an alternative to the above style of reference, an alphanumeric code may be used in place of the number (e.g., [A<sup>U</sup>Th90]). The same commands are used, but `\bibitem` takes an optional argument containing the desired alphanumeric code.

Another alternative is no number, simply the authors' names and the year of publication following in parentheses. The rest of the format is identical. The macros do not support this alternative directly, but modifications to the macro definition are possible if this reference style is preferred.

**8. Conclusion.** Many other style suggestions and tips could be given to help authors but are beyond the scope of this document. Simple mistakes can be avoided by increasing your familiarity with how L<sup>A</sup>T<sub>E</sub>X functions. The books referred to throughout this document are also useful to the author who wants clear, beautiful typography with minimal mistakes.

**Appendix. The use of appendices.** The `\appendix` command may be used before the final sections of a paper to designate them as appendices. Once `\appendix` is called, all subsequent sections will appear as

**Appendix A. Title of appendix.** Each one will be sequentially lettered instead of numbered. Theorem-like environments, subsections, and equations will also have the section number changed to a letter.

If there is only *one* appendix, however, the `\Appendix` (with a capital letter) should be used instead. This produces only the word **Appendix** in the section title, and does not add a letter. Equation numbers, theorem numbers and subsections of the appendix will have the letter "A" designating the section number.

If you don't want to title your appendix, and just call it **Appendix A.** for example, use `\appendix\section*{}` and don't include anything in the title field. This works opposite to the way `\section*` usually works, by including the section number, but not using a title.

Appendices should appear before the bibliography section, not after, and any acknowledgments should be placed after the appendices and before the bibliography.

## REFERENCES

- [1] M. GOOSSENS, F. MITTELBACH, AND A. SAMARIN, *The L<sup>A</sup>T<sub>E</sub>X Companion*, Addison-Wesley, Reading, MA, 1994.
- [2] N. J. HIGHAM, *Handbook of Writing for the Mathematical Sciences*, Society for Industrial and Applied Mathematics, Philadelphia, PA, 1993.
- [3] L. LAMPORT, *L<sup>A</sup>T<sub>E</sub>X: A Document Preparation System*, Addison-Wesley, Reading, MA, 1986.
- [4] R. SEROUL AND S. LEVY, *A Beginner's Book of T<sub>E</sub>X*, Springer-Verlag, Berlin, New York, 1991.



# Recovery algorithms for vector valued data with joint sparsity constraints

Massimo Fornasier<sup>†</sup> and Holger Rauhut<sup>‡</sup>

August 2006

## Abstract

Vector valued data appearing in concrete applications often possess sparse expansions with respect to a preassigned frame for each vector component individually. Additionally, different components may also exhibit common sparsity patterns. Recently, there were introduced sparsity measures that take into account such joint sparsity patterns, promoting coupling of non-vanishing components. These measures are typically constructed as weighted  $\ell_1$  norms of componentwise  $\ell_q$  norms of frame coefficients. We show how to compute solutions of linear inverse problems with such joint sparsity regularization constraints by fast thresholded Landweber algorithms. Next we discuss the adaptive choice of suitable weights appearing in the definition of sparsity measures. The weights are interpreted as indicators of the sparsity pattern and are iteratively updated after each new application of the thresholded Landweber algorithm. The resulting two-step algorithm is interpreted as a double-minimization scheme for a suitable target functional. We show its  $\ell_2$ -norm convergence. An implementable version of the algorithm is also formulated, and its norm convergence is proven. Numerical experiments in color image restoration are presented.

**AMS subject classification:** 65J22, 65K10, 65T60, 90C25, 52A41, 49M30, 68U10

**Key Words:** linear inverse problems, joint sparsity, thresholded Landweber iterations, curvelets, subdifferential inclusion, color image reconstruction

## 1 Introduction

**Inverse problems.** We address the problem of recovering an element  $u$  of a Hilbert space  $\mathcal{K}$  from the observed datum  $g = Tu$  in the Hilbert space  $\mathcal{H}$ , where  $T : \mathcal{K} \rightarrow \mathcal{H}$  is a bounded linear operator, possibly non-invertible or with unbounded inverse. A simple approach to this problem is to minimize the discrepancy

$$\mathcal{T}(u) := \|Tu - g\|_{\mathcal{H}}^2.$$

---

<sup>†</sup>Johann Radon Institute for Computational and Applied Mathematics, Austrian Academy of Sciences, Altenbergerstrasse 69, A-4040 Linz, Austria, [massimo.fornasier@oeaw.ac.at](mailto:massimo.fornasier@oeaw.ac.at)  
MF acknowledges the financial support provided by the European Union's Human Potential Programme under contract MEIF-CT-2004-501018. He also thanks NuHAG for its warm hospitality.

<sup>‡</sup>Numerical Harmonic Analysis Group, Faculty of Mathematics, University of Vienna, Nordbergstrasse 15, A-1090 Vienna, Austria, [holger.rauhut@univie.ac.at](mailto:holger.rauhut@univie.ac.at)  
HR acknowledges the financial support provided by the European Union's Human Potential Programme under contracts HPRN-CT-2002-00285 (HASSIP) and MEIF-CT-2006-022811.

If  $\ker(T) = \{0\}$  then there exists a unique solution given by  $u^* = (T^*T)^{-1}T^*g$ . However, if  $T$  has unbounded inverse, i.e.,  $(T^*T)^{-1}$  is unbounded then this approach is very unstable.

Thus, if  $T$  is non-invertible or has unbounded inverse (or an inverse with high norm) one has to take into account further features of the expected solution. Indeed, a well-known way out is to consider the regularized problem [26]

$$u_\alpha^* := \operatorname{argmin}_{u \in \mathcal{K}} \mathcal{T}(u) + \alpha \|u|_{\mathcal{K}}\|^2.$$

for which the corresponding solution operator  $T_\alpha^\dagger : g \mapsto u_\alpha^*$  is bounded. Unfortunately, the minimal norm constraint is often not appropriate. A recent approach is to substitute this particular constraint with a more general one

$$u_\Phi^* := \operatorname{argmin}_{u \in \mathcal{K}} \mathcal{T}(u) + \Phi(u),$$

where  $\Phi$  is a suitable *sparsity measure*.

**Sparse frame expansions.** A *sparse representation* of an element of a Hilbert space is a series expansion with respect to an orthonormal bases or a frame that has only a small number of large coefficients. Several types of signals appearing in nature admit sparse frame expansions and thus, sparsity is a realistic assumption for a very large class of problems. For instance, images are well-represented by sparse expansions with respect to wavelets or curvelets, while for audio signals a Gabor frame is a good choice.

Sparsity has had already a long history of successes. The design of frames for sparse representations of digital signals has led to extremely efficient compression methods, such as JPEG2000 and MP3 [33]. Successively a new generation of optimal numerical schemes has been developed for the computation of sparse solutions of differential and integral equations, exploiting adaptive and greedy strategies [12, 38, 14, 15]. The use of sparsity in inverse problems for data recovery has been the most recent step of this long career of “simplifying and understanding complexity”, with an enormous potential in applications [2, 17, 18, 20, 22, 21, 35, 39, 10, 13, 16]. Another field, which caught much attention recently, is the observation that it is possible to reconstruct sparse signals from vastly incomplete information [7, 6, 23, 32, 36]. This line of research is called sparse recovery or compressed sensing.

**From sparsity to joint sparsity.** Most of the contributions appearing in the literature are addressed to the recovery of sparse scalar functions. Multi-channel signals (i.e., vector valued functions) appearing in concrete applications may not only possess sparse frame expansions for each channel individually, but additionally the different channels can also exhibit common sparsity patterns. Recently, new sparsity measures have been introduced that promote such coupling of the non-vanishing components through different channels [3, 29, 40]. These measures are typically constructed as *weighted*  $\ell_1$  norms of channel  $\ell_q$  norms with  $q > 1$ . We will use this concept for the solution of vector valued inverse problems and combine it with another approach further promoting the coupling of sparsity patterns along channels.

**Our main results.** We show how to compute solutions of linear inverse problems with joint sparsity regularization constraints by fast thresholded Landweber algorithms, similar to those presented in [17, 35, 39]. We discuss the adaptive choice of suitable *weights* appearing in the definition of the sparsity measures. The *weights* are interpreted as indicators of the sparsity pattern and are iteratively up-dated after each new application of

the thresholded Landweber algorithm. The resulting two-step algorithm is interpreted as a double-minimization scheme for a suitable target functional. We prove that our algorithm converges to its minimizer. Since the functional is not smooth, this is done by subdifferential inclusions [37]. We prove that the thresholded Landweber algorithm, which constitutes the inner iteration of the double-minimization algorithm, converges linearly. This feature was not ensured by the versions in [17, 39]. The second step of the double-minimization has actually a simple explicit solution. Finally, we show that the full exact double-minimization scheme converges linearly and we provide an implementable version which is also ensured to converge.

**Morphological analysis of signals and sparsity patterns.** The use of sparseness measures not only allows to reconstruct a signal. At the same time it gives information about (joint) sparsity patterns which may encode morphological features of the signal. Well-known examples are the microlocal analysis properties of wavelets [30, 31] for singularity and regularity detection, and the characterization of edges and curves by curvelets for natural images [9]. For instance, the weight sequences appearing in the sparsity measures we define, and interpreted as indicators of the sparsity pattern, play a similar role as the discontinuity set is playing in the Mumford-Shah functional [34]. In fact, it is well-known that wavelet or curvelet coefficients have high absolute values at high scales as soon as we are in the neighborhood of discontinuities. Even more illuminating and suggestive is the parallel between the sparsity measure and its indicator weights with the Ambrosio-Tortorelli [1] approximation of the Mumford-Shah functional. Here, the discontinuity set is indicated by an auxiliary function which is 1 where the image is smooth and 0 where edges and discontinuities are detected.

Joint sparsity patterns of vector valued (i.e., multi-channel) signals encode even finer properties of the morphology which do not belong only to one channel but are a common feature of all the channels. Here the parallel is with generalizations of the Mumford-Shah functional as appearing for example in [5] where polyconvex functions of gradients couple discontinuity sets through different color channels of images.

**Applications.** We expect that our scheme can be applied in several different contexts. In this paper we limit ourselves to an application in color image reconstruction, modeling a real-world problem in art restoration. Indeed, color images have the advantage to be non-trivial multivariate and multi-channel signals, exhibiting a very rich morphology and structure. In particular, discontinuities (jump sets) may appear in all the channels at the same locations, which will be reflected in their curvelet representation (for instance). For these reasons, color images are a good model to test the effectiveness of our scheme promoting joint sparsity, also because the solution can be easily checked just by a visual analysis. Of course, the range of applicability of our approach is not limited to color image restoration. Neuroimaging (functional Magnetic Resonance Imaging, Magnetoencephalography), distributed compressed sensing [3] and several other problems with coupled vector valued solutions are fields where we expect that our scheme can be fruitfully used. The numerical solution of differential and integral operator equations can also be addressed within this framework and we refer for example to [14, 38, 15] for implementations by adaptive strategies.

**Content of the paper.** The paper is organized as follows. In Section 2 we introduce the mathematical setting. We formulate our model of joint sparsity for multi-channel signals

and the corresponding functional to be minimized in order to solve a given linear inverse problem. The functional depends on two variables. The first belongs to the space of signals to be reconstructed, the second belongs to the space of sparsity indicator weights. Convexity properties of the functional are discussed. Section 3 is dedicated to the formulation of the double-minimization algorithm and to its weak-convergence. The scheme is based on alternating minimizations in the first and in the second variable individually. In Section 4 we discuss an efficient thresholded Landweber algorithm for the minimization with respect to the first variable. Its strong convergence is shown following the analysis in [17]. The minimization with respect to the second variable has an explicit solution and no elaboration is needed. We provide an implementable version of the full scheme in Section 5. To prove its convergence we develop an error analysis. As a byproduct of the results in this section we show that the double-minimization scheme converges strongly. In Section 6 we present an application in color image reconstruction. Numerical experiments are shown and discussed.

## Nota on color pictures

This paper introduces methods to recover colors in digital images. Therefore a gray level printout of the manuscript does not allow to appreciate fully the quality of the illustrated techniques. The authors recommend the interested reader to access the electronic version with color pictures which is available online.

## 2 The Functional

### 2.1 Notation

Before starting our discussion let us briefly introduce some of the spaces we will use in the following. For some countable index set  $\Lambda$  we denote by  $\ell_p = \ell_p(\Lambda)$ ,  $1 \leq p \leq \infty$ , the space of real sequences  $u = (u_\lambda)_{\lambda \in \Lambda}$  with norm

$$\|u\|_p = \|u\|_{\ell_p} := \left( \sum_{\lambda \in \Lambda} |u_\lambda|^p \right)^{1/p}, \quad 1 \leq p < \infty$$

and  $\|u\|_\infty := \sup_{\lambda \in \Lambda} |u_\lambda|$  as usual. If  $(v_\lambda)$  is a sequence of positive weights then we define the weighted spaces  $\ell_{p,v} = \ell_{p,v}(\Lambda) = \{u, (u_\lambda v_\lambda) \in \ell_p(\Lambda)\}$  with norm

$$\|u\|_{p,v} = \|u\|_{\ell_{p,v}} = \|(u_\lambda v_\lambda)\|_p = \left( \sum_{\lambda \in \Lambda} v_\lambda^p |u_\lambda|^p \right)^{1/p}$$

(with obvious modification for  $p = \infty$ ). If the entries  $u_\lambda$  are actually vectors in a Banach space  $X$  with norm  $\|\cdot\|_X$  then we denote

$$\ell_{p,v}(\Lambda, X) := \{(u_\lambda)_{\lambda \in \Lambda}, u_\lambda \in X, (\|u_\lambda\|_X)_{\lambda \in \Lambda} \in \ell_{p,v}(\Lambda)\}$$

with norm  $\|u\|_{\ell_{p,v}(\Lambda, X)} = \|(\|u_\lambda\|_X)_{\lambda \in \Lambda}\|_{\ell_{p,v}(\Lambda)}$ . Usually  $X$  will be  $\mathbb{R}^M$  endowed with the Euclidean norm, or the  $M$ -dimensional space  $\ell_q^M$ , i.e.,  $\mathbb{R}^M$  endowed with the  $\ell_q$ -norm. By  $\mathbb{R}_+$  we denote the non-negative real numbers.

## 2.2 Inverse Problems with joint sparsity constraints

Let  $\mathcal{K}$  and  $\mathcal{H}_j$ ,  $j = 1, \dots, N$ , be (separable) Hilbert spaces and  $A_{\ell,j} : \mathcal{K} \rightarrow \mathcal{H}_j$ ,  $j = 1, \dots, M$ ,  $\ell = 1, \dots, N$ , some bounded linear operators. Assume we are given data  $g_j \in \mathcal{H}_j$ ,

$$g_j = \sum_{\ell=1}^M A_{\ell,j} f_\ell, \quad j = 1, \dots, N.$$

Then our basic task consists in reconstructing the (unknown) elements  $f_\ell \in \mathcal{K}$ ,  $\ell = 1, \dots, M$ .

In practice, it happens that the corresponding mapping from the vector  $(f_\ell)$  to the vector  $(g_j)$  is not invertible or ill-conditioned. Moreover, the data  $g_j$ ,  $j = 1, \dots, N$ , are often corrupted by noise. Thus, in order to deal with our reconstruction problem we have to regularize it.

Our basic assumption throughout this paper will be that the 'channels'  $f_\ell$ ,  $\ell = 1, \dots, M$ , are correlated by means of joint sparsity patterns. Our aim is to model the joint sparsity within a regularization term. In the following we develop this idea.

For the sake of short notation we resume the data vector into

$$g = (g_j)_{j=1, \dots, M} \in \mathcal{H} := \bigoplus_{j=1}^N \mathcal{H}_j$$

where the Hilbert space  $\mathcal{H}$  is equipped with the usual inner product  $\langle \sum_j g_j, \sum_j h_j \rangle := \sum_j \langle g_j, h_j \rangle$  with  $g_j, h_j \in \mathcal{H}_j$ . We also combine the operators  $A_{\ell,j}$  into one operator

$$A : \bigoplus_{\ell=1}^M \mathcal{K} \rightarrow \mathcal{H}, \quad A(f_\ell)_{\ell=1}^M = \left( \sum_{\ell=1}^M A_{\ell,j} f_\ell \right)_{j=1}^N.$$

In order to exploit sparsity ideas we assume that we have given a suitable frame  $\{\psi_\lambda : \lambda \in \Lambda\} \subset \mathcal{K}$  indexed by a countable set  $\Lambda$ . This means that there exist constants  $C_1, C_2 > 0$  such that

$$C_1 \|f\|_{\mathcal{K}}^2 \leq \sum_{\lambda \in \Lambda} |\langle f, \psi_\lambda \rangle|^2 \leq C_2 \|f\|_{\mathcal{K}}^2 \quad \text{for all } f \in \mathcal{K}. \quad (1)$$

Orthonormal bases are particular examples of frames. Frames allow for a (stable) series expansion of any  $f \in \mathcal{K}$  of the form

$$f = Fu := \sum_{\lambda \in \Lambda} u_\lambda \psi_\lambda \quad (2)$$

where  $u = (u_\lambda)_{\lambda \in \Lambda} \in \ell_2(\Lambda)$ . The linear operator  $F : \ell_2(\Lambda) \rightarrow \mathcal{K}$  is called the *synthesis map* in frame theory. It is bounded due to the frame inequality (1). In contrast to orthonormal bases, the coefficients  $u_\lambda$  need not be unique, in general. For more information on frames we refer to [11].

A main assumption here is that the  $f_\ell$  to be reconstructed are sparse with respect to the frame  $\{\psi_\lambda\}$ . This means that  $f_\ell$  can be well-approximated by a series of the form (2) with only a small number of non-vanishing coefficients  $u_\lambda$ . This can be modelled by assuming

that the sequence  $u$  is contained in a (weighted)  $\ell_1(\Lambda)$ -space. Indeed, the minimization of the  $\ell_1(\Lambda)$  norm promotes that only few entries are non-zero. Taking for instance a wavelet frame and a suitable weight, the  $\ell_1$  constraint implies that the element to be reconstructed lies in a certain Besov space  $B_{1,1}^s$ , see [17].

Analogously as in [17] such considerations lead to the regularized functional

$$\mathcal{J}(u) = \|g - Tu\|_{\mathcal{H}}^2 + \|u\|_{\ell_{1,v}(\Lambda^M)} = \sum_{j=1}^N \left\| g_j - \sum_{\ell=1}^M A_{\ell,j} F u^\ell \right\|_{\mathcal{H}_j}^2 + \sum_{\ell=1}^M \sum_{\lambda \in \Lambda} v_\lambda |u_\lambda^\ell|, \quad (3)$$

which has to be minimized with respect to the vector of coefficients  $u = (u_\lambda^\ell)_{\lambda \in \Lambda}^{\ell=1, \dots, M}$ . The  $\ell_{1,v}$  norm in this functional clearly represents the regularization term. The numbers  $v_\lambda$ ,  $\lambda \in \Lambda$ , are some suitable positive weights. Once the minimizer  $u = (u_\lambda^\ell)$  is determined we obtain a reconstruction of the vectors of interest by means of  $f_\ell = F u^\ell = \sum_{\lambda} u_\lambda^\ell \psi_\lambda$ . The algorithm in [17] can be taken to perform the minimization with respect to  $u$ .

The functional  $\mathcal{J}(u)$  in the form stated, however, does not necessarily model any correlation between the vectors ('channels')  $f_\ell$ ,  $\ell = 1, \dots, M$ . A way to incorporate such correlation is the assumption of joint sparsity, see also [29, 40]. By this we mean that the pattern of non-zero coefficients representing  $f_\ell$  is (approximately) the same for all the channels. In other words, for some *finite* set of indexes  $\Lambda_0 \subset \Lambda$  and for all  $\ell = 1, \dots, M$  there is an expansion

$$f_\ell \approx \sum_{\lambda \in \Lambda_0} u_\lambda^\ell \psi_\lambda.$$

In particular, the *same*  $\Lambda_0$  can be chosen for all  $f_\ell$ 's.

We propose two approaches (that can be combined) to model joint sparsity. The first one assumes that the mixed norm

$$\|u\|_{\ell_{1,v}(\Lambda, \ell_q^M)} = \sum_{\lambda \in \Lambda} v_\lambda \|u_\lambda\|_q$$

of  $u = (u_\lambda^\ell)$  is small. Hereby,  $u_\lambda$  denotes the vector  $(u_\lambda^\ell)_{\ell=1}^M$  in  $\mathbb{R}^M$ . (Recall also that  $\ell_q^M$  denotes  $\mathbb{R}^M$  endowed with the  $\ell_q$ -norm). Here,  $q > 1$  and in particular,  $q = 2$  or  $q = \infty$ , represent the interesting cases, since for  $q = 1$  the above norm reduces to the usual weighted  $\ell_{1,v}$  norm. In fact if  $q$  is large and some  $|u_\lambda^\ell|$  is large then the channel entries  $|u_\lambda^{\ell'}|$  are also allowed to be large for  $\ell' \neq \ell$ , without increasing significantly the norm  $\|u_\lambda\|_{\ell_q^M}$ . The minimization of the above norm promotes that all entries of the 'interchannel' vector  $u_\lambda$  may become significant, once at least one of the components  $|u_\lambda^\ell|$  is large.

Introduce the operators  $T_{\ell,j} = A_{\ell,j} F : \ell_2(\Lambda) \rightarrow \mathcal{H}_\ell$  and

$$T : \ell_2(\Lambda, \mathbb{R}^M) \rightarrow \mathcal{H}, \quad Tu = \left( \sum_{\ell=1}^M T_{\ell,j} u^\ell \right)_{j=1}^N = \left( \sum_{\ell=1}^M A_{\ell,j} F u^\ell \right)_{j=1}^N.$$

The above reasoning leads to the functional

$$\begin{aligned} K(u) &= K_v^{(q)}(u) := \|Tu - g\|_{\mathcal{H}}^2 + \|u\|_{\ell_{1,v}(\Lambda, \ell_q^M)} \\ &= \sum_{j=1}^N \left\| \sum_{\ell=1}^M T_{\ell,j} u^\ell - g_j \right\|_{\mathcal{H}_j}^2 + \sum_{\lambda \in \Lambda} v_\lambda \|u_\lambda\|_q \end{aligned} \quad (4)$$

to be minimized with respect to  $u$ . In Section 4 we will develop an iterative thresholding algorithm similar as in [17] to perform this minimization.

The second approach to support joint sparsity is to encode the joint sparsity information in some sort of indicator function. This can in fact be done by using the weight  $(v_\lambda)$  as a second minimization variable. To this end we add an additional term to the original functional (3), punishing small values of  $v_\lambda$ . We obtain the functional

$$J_0(u, v) := J_{\theta, \rho, 0}^{(1)}(u, v) := \|Tu - g|\mathcal{H}\|^2 + \sum_{\lambda \in \Lambda} v_\lambda \|u_\lambda\|_1 + \sum_{\lambda} \theta_\lambda (\rho_\lambda - v_\lambda)^2$$

restricted to  $v_\lambda \geq 0$ . Here,  $(\theta_\lambda)_\lambda$  and  $(\rho_\lambda)_\lambda$  are some suitable positive sequences.

Now the task is to minimize  $J_0(u, v)$  jointly with respect to both  $u, v$ . (Again, once this minimizer is determined we obtain  $f_\ell = Fu^\ell$ ). Analyzing  $J_0(u, v)$  we realize that for the minimizer  $(u, v)$  we will have  $v_\lambda = 0$  (or close to 0) if  $\|u_\lambda\|_1 = \sum_{\ell=1}^M |u_\lambda^\ell|$  is large so that  $v_\lambda \|u_\lambda\|_1$  gets small. On the other hand, if  $\|u_\lambda\|_1$  is small then the term  $\theta_\lambda (\rho_\lambda - v_\lambda)$  dominates and forces  $v_\lambda$  to be close to  $\rho_\lambda$ . Thus,  $v_\lambda$  serves indeed as an indicator of large values of  $\|u_\lambda\|_1$ . It has the effect, that if  $v_\lambda$  is chosen small due to one large  $u_\lambda^\ell$  then also the other coefficients  $u_\lambda^{\ell'}, \ell' \neq \ell$  can be chosen large without making the functional considerably bigger.

Unfortunately, in contrast to the previous functionals,  $J(u, v)$  as stated above is no longer jointly convex in  $(u, v)$  in general (although it is convex as functional of  $u$  and of  $v$  alone). Thus, it cannot be ensured that a local minimum of the functional will be a global one, a property that is very crucial for an efficient minimization method.

To overcome this problem we may add an additional suitable quadratic term. Moreover, we can, of course, combine the second approach with the first one and use an  $\ell_q$ -norm instead of an  $\ell_1$ -norm for the 'interchannel' vectors  $u_\lambda$ . This leads to the most general form of the regularized functional considered in this paper,

$$J(u, v) = J_{\theta, \rho, \omega}^{(q)}(u, v) := \|Tu - g|\mathcal{H}\|^2 + \sum_{\lambda \in \Lambda} v_\lambda \|u_\lambda\|_q + \sum_{\lambda \in \Lambda} \omega_\lambda \|u_\lambda\|_2^2 + \sum_{\lambda \in \Lambda} \theta_\lambda (\rho_\lambda - v_\lambda)^2. \quad (5)$$

Here,  $\omega_\lambda$  is a suitably chosen sequence of positive numbers, and  $1 \leq q \leq \infty$ .

We will provide a sufficient condition depending on  $\theta_\lambda$  and  $\rho_\lambda$  in the next subsection ensuring the strict joint convexity of  $J(u, v)$  in  $(u, v)$ . Although there is an extra term,  $J(u, v)$  has similar properties as  $J_0(u, v)$ . In particular,  $v$  can still be seen as a sort of indicator function.

Observe that in the minimum we will always have  $0 \leq v_\lambda \leq \rho_\lambda$ . Therefore, we can assume the domain of  $J$  to be  $\ell_2(\Lambda, \mathbb{R}^M) \times \ell_{\infty, \rho^{-1}}(\Lambda)_+$  where  $\ell_{\infty, \rho^{-1}}(\Lambda)_+$  denotes the (convex) cone of all non-negative sequences  $(v_\lambda) \in \ell_{\infty, \rho^{-1}}(\Lambda)$ .

Our main contribution consists in providing an algorithm for the minimization of  $J(u, v)$ . It consists in alternately minimizing with respect to  $u$  and with respect  $v$ . The minimization with respect to  $v$  can be done explicitly. For the minimization with respect to  $u$  we propose an efficient iterative algorithm.

We will mainly study the problem in the real-valued case. The complex-valued case can be treated with the same methods (in principle) by observing that  $\mathbb{C}^M$  is isomorphic to

$\mathbb{R}^{2M}$ , so passing from  $M$  complex-valued channels to  $2M$  real-valued channels. We note, however, that slight complications may arise from the fact that an  $\ell_q$  norm on  $\mathbb{C}^M$  is not isometric to an  $\ell_q$ -norm on  $\mathbb{R}^{2M}$  if  $q \neq 2$ . (In particular, the thresholding operator on  $\mathbb{C}^M$  for  $q = \infty$  will have a different form than the one provided in the next Section for the real-valued case).

### 2.3 Convexity of the functional $J$

At several places in the following it will be convenient to write

$$J(u, v) = \mathcal{T}(u) + \Phi^{(q)}(u, v) \quad (6)$$

where

$$\begin{aligned} \mathcal{T}(u) &= \|Tu - g\|_{\mathcal{H}}^2 = \sum_{j=1}^N \left\| \sum_{\ell=1}^M T_{\ell,j} u^\ell - g_j \right\|_{\mathcal{H}_j}^2 \\ \Phi^{(q)}(u, v) &= \sum_{\lambda \in \Lambda} v_\lambda \|u_\lambda\|_q + \sum_{\lambda \in \Lambda} \omega_\lambda \|u_\lambda\|_2^2 + \sum_{\lambda \in \Lambda} \theta_\lambda (\rho_\lambda - v_\lambda)^2 \\ &= \|(v_\lambda \|u_\lambda\|_q)_{\lambda \in \Lambda}\|_1 + \left\| |u|_{\ell_{2,\omega^{1/2}}(\Lambda, \ell_2^M)} \right\|^2 + \|\rho - v\|_{\ell_{2,\theta^{1/2}}(\Lambda)}^2, \end{aligned}$$

are the discrepancy with respect to the data and the joint sparsity measure, respectively.

Also it is useful to observe that  $\Phi^{(q)}$  decouples with respect to  $\lambda$ , i.e.,

$$\Phi^{(q)}(u, v) = \sum_{\lambda \in \Lambda} \Phi_\lambda^{(q)}(u_\lambda, v_\lambda) \quad (7)$$

where

$$\begin{aligned} \Phi_\lambda^{(q)}(x, y) &= y \|x\|_q + \omega_\lambda \|x\|_2^2 + \theta_\lambda (\rho_\lambda - y)^2 \\ &= y \left( \sum_{\ell=1}^M |x_\ell|^q \right)^{1/q} + \omega_\lambda \sum_{\ell=1}^M x_\ell^2 + \theta_\lambda (\rho_\lambda - y)^2, \quad x \in \mathbb{R}^M, y \geq 0 \end{aligned} \quad (8)$$

(with the usual modification for  $q = \infty$ ).

In the following we give necessary and sufficient conditions for the (strict) convexity of the functional  $\Phi^{(q)}$  for the most interesting cases  $q = 1, 2, \infty$ . These imply sufficient conditions for the (strict) convexity of  $J = J_{\theta, \rho, \omega}^{(q)}$ .

**Proposition 2.1.** *Let  $q \in \{1, 2, \infty\}$ . The sparsity measure  $\Phi^{(q)}$  is convex if and only if  $\omega_\lambda \theta_\lambda \geq \frac{\kappa}{4}$  for all  $\lambda \in \Lambda$ , where  $\kappa = M$  for  $q = 1$ , and  $\kappa = 1$  for  $q \in \{2, \infty\}$ . In particular, if  $\omega_\lambda \theta_\lambda \geq \frac{\kappa}{4}$  for all  $\lambda \in \Lambda$  then  $J$  is convex. In case of a strict inequality  $\omega_\lambda \theta_\lambda > \frac{\kappa}{4}$  we can replace “convexity” by “strict convexity” in all of these statements.*

*Proof.* It is easy to see that  $\Phi^{(q)}$  is (strictly) convex if and only if all the  $\Phi_\lambda^{(q)}$ ,  $\lambda \in \Lambda$ , are (strictly) convex.



Let us first consider  $q = 1$ . Observe that we can write  $\Phi_\lambda^{(1)}(x, y) = \sum_{\ell=1}^M F_\lambda^{(1)}(x_\ell, y)$  with

$$\begin{aligned} F_\lambda^{(1)}(z, y) &= y|z| + \omega_\lambda |z|^2 + M^{-1}\theta_\lambda(\rho_\lambda - y)^2 \\ &= (y|z| + \omega_\lambda |z|^2 + M^{-1}\theta_\lambda y^2) + (\rho_\lambda^2 - 2\theta_\lambda y), \quad z \in \mathbb{R}, y \geq 0. \end{aligned} \quad (9)$$

The function in the second bracket is obviously linear, hence convex. The function in the first bracket can be written as the composition  $G_\lambda \circ L$  with  $L(z, y) = (|z|, y)$  and

$$G_\lambda(z, y) = yz + \omega_\lambda z^2 + M^{-1}\theta_\lambda y^2 = \frac{1}{2}(z, y) H^{(1)}(z, y)^T, \quad z, y \in \mathbb{R},$$

where

$$H^{(1)} = \begin{pmatrix} 2\omega_\lambda & 1 \\ 1 & 2\theta_\lambda M^{-1} \end{pmatrix}.$$

Since  $L$  is convex and has range  $\mathbb{R}_+^2$ , and  $G_\lambda$  is monotonically increasing in each coordinate on  $\mathbb{R}_+^2$  it suffices to show that  $G_\lambda(z, y)$  is convex if and only if  $\theta_\lambda \omega_\lambda \geq M/4$ , see e.g. [4, p. 86]. The convexity of  $G_\lambda$  is equivalent to  $H^{(1)}$  being positive semidefinite. The latter is clearly equivalent to  $\theta_\lambda \omega_\lambda \geq M/4$ . Strict convexity is equivalent to a strict inequality  $\theta_\lambda \omega_\lambda > M/4$ .

Now let  $q = 2$ . Observe that  $\Phi_\lambda^{(2)} = F_\lambda^{(2)} \circ L^{(2)}$  where  $L^{(2)} : \mathbb{R}^M \times \mathbb{R}_+ \rightarrow \mathbb{R}_+^2$ ,  $L^{(2)}(x, y) = (\|x\|_2, y)$  and

$$F_\lambda^{(2)}(z, y) = yz + \omega_\lambda z^2 + \theta_\lambda(\rho_\lambda - y)^2 = \frac{1}{2}(z, y) H^{(2)}(z, y)^T + \theta_\lambda(\rho_\lambda^2 - 2\rho_\lambda y), \quad z, y \in \mathbb{R} \quad (10)$$

with

$$H^{(2)} = \begin{pmatrix} 2\omega_\lambda & 1 \\ 1 & 2\theta_\lambda \end{pmatrix}.$$

By a similar argument as above  $\Phi_\lambda^{(2)}$  is convex if and only if  $H^{(2)}$  is positive semi-definite. The latter is the case if and only if  $\omega_\lambda \theta_\lambda \geq 1/4$ , and strict convexity is equivalent to a strict inequality.

Finally, let  $q = \infty$ . Observe that

$$\Phi_\lambda^{(\infty)}(x, y) = \max_{\ell=1, \dots, M} \left\{ y|x_\ell| + \omega_\lambda \sum_{m=1}^M |x_m|^2 + \theta_\lambda(\rho_\lambda - y)^2 \right\}.$$

Since  $\Phi_\lambda^{(\infty)}$  is the pointwise maximum of  $M$  functions, it is sufficient (see [4, p. 80]) to investigate the (strict) convexity of each of the functions

$$\begin{aligned} f_{\lambda, \ell}(x, y) &= yx_\ell + \omega_\lambda \sum_{m=1}^M (x_m)^2 + \theta_\lambda(\rho_\lambda - y)^2 \\ &= \frac{1}{2}(y, x) H_\ell^{(\infty)}(y, x)^T + \theta_\lambda(\rho_\lambda^2 - 2y\rho_\lambda), \quad x \in \mathbb{R}^M, y \geq 0, \end{aligned}$$

with

$$H_\ell^{(\infty)} = \begin{pmatrix} 2\omega_\lambda & 0 & \cdots & 0 & \delta_{1,\ell} \\ 0 & 2\omega_\lambda & \cdots & 0 & \delta_{2,\ell} \\ \vdots & \vdots & \ddots & \vdots & \vdots \\ 0 & 0 & \cdots & 2\omega_\lambda & \delta_{M,\ell} \\ \delta_{1,\ell} & \delta_{2,\ell} & \cdots & \delta_{M,\ell} & 2\theta_\lambda \end{pmatrix}.$$

One can show by induction that

$$\det(H_\ell^{(\infty)}) = 2^{M-1}\omega_\lambda^{M-1}(4\theta_\lambda\omega_\lambda - 1).$$

Thus,  $H_\ell^{(\infty)}$  is positive semidefinite if and only if  $\theta_\lambda\omega_\lambda \geq 1/4$ , and the convexity of  $\Phi_\lambda^{(q)}$  is equivalent to the latter condition. Once again strict convexity is equivalent to the strict inequality.  $\square$

We do not pursue the task to obtain conditions for the convexity of  $\Phi^{(q)}$  and  $J$  for general  $q \neq 1, 2, \infty$ , but rather assume that  $\Phi^{(q)}$  and hence  $J$  are always convex also in this case.

### 3 The Minimizing Algorithm and its Convergence

In this section we propose and analyze an algorithm for the computation of the minimizer  $(u^*, v^*)$  of the functional  $J(u, v) = J_{\theta, \rho, \omega}^{(q)}(u, v)$  defined in (5). The algorithm consists in alternating a minimization with respect to  $u$  and a minimization with respect to  $v$ . More formally, for some initial choice  $v^{(0)}$ , for example  $v^{(0)} = (\rho_\lambda)_{\lambda \in \Lambda}$ , we define

$$\begin{aligned} u^{(n)} &:= \arg \min_{u \in \ell_2(\Lambda, \mathbb{R}^M)} J(u, v^{(n-1)}), \\ v^{(n)} &:= \arg \min_{v \in \ell_{\infty, \rho^{-1}}(\Lambda)_+} J(u^{(n)}, v). \end{aligned} \quad (11)$$

The minimization of  $J(u, v^{(n-1)})$  with respect to  $u$  can be done by means of the iterative thresholding algorithm that we will study in the next section. The minimizer  $v^{(n)}$  of  $J(u^{(n)}, v)$  for fixed  $u^{(n)}$  can be computed explicitly. Indeed, it follows from elementary calculus that

$$v_\lambda^{(n)} = \begin{cases} \rho_\lambda - \frac{1}{2\theta_\lambda} \|u^{(n)}\|_q & \text{if } \|u^{(n)}\|_q < 2\theta_\lambda \rho_\lambda \\ 0 & \text{otherwise.} \end{cases} \quad (12)$$

We have the following result about the convergence of the above algorithm.

**Theorem 3.1.** *Let  $1 \leq q \leq \infty$  and assume that  $\Phi^{(q)}$  and hence  $J$  are strictly convex (see also Proposition 2.1). Moreover, we assume that  $\ell_{2, \omega^{1/2}}(\Lambda, \mathbb{R}^M)$  is embedded into  $\ell_2(\Lambda, \mathbb{R}^M)$ , i.e.,  $\omega_\lambda \geq \gamma > 0$  for all  $\lambda \in \Lambda$ . Then the sequence  $(u^{(n)}, v^{(n)})_{n \in \mathbb{N}}$  converges to the unique minimizer  $(u^*, v^*) \in \ell_2(\Lambda, \mathbb{R}^M) \times \ell_{\infty, \rho^{-1}}(\Lambda)_+$  of  $J$ . The convergence of  $u^{(n)}$  is weak in  $\ell_2(\Lambda, \mathbb{R}^M)$  and that of  $v^{(n)}$  holds componentwise.*

*For the most interesting cases  $q \in \{1, 2, \infty\}$ , if in addition  $\theta_\lambda \omega_\lambda \geq \sigma > \phi_q/4$  for all  $\lambda \in \Lambda$ , where  $\phi_1 = M$ ,  $\phi_2 = 1$ ,  $\phi_\infty = \sqrt{M}$  then the convergence of  $u^{(n)}$  to  $u^*$  is also strong in  $\ell_2(\Lambda, \mathbb{R}^M)$  and  $v^{(n)} - v^*$  converges to 0 strongly in  $\ell_{2, \theta}(\Lambda)$ .*

The rest of the section will be spent with the proof of the weak convergence of the algorithm. The strong convergence and the full proof of the Theorem 3.1 will be established only in Subsection 5.3 later.

### 3.1 Subdifferential calculus

A main tool in the analysis of non-smooth functionals and their minima is the concept of subdifferential. Recall that for a convex functional  $F$  on some Banach space  $V$  its subdifferential  $\partial F(x)$  at a point  $x \in V$  with  $F(x) < \infty$  is defined as the set

$$\partial F(x) = \{x^* \in V^*, x^*(z - x) + F(x) \leq F(z) \text{ for all } z \in V\},$$

where  $V^*$  denotes the dual space of  $V$ . It is obvious from this definition that  $0 \in \partial F(x)$  if and only if  $x$  is a minimizer of  $F$ . In the following we investigate the subdifferential of  $J$ . In order to have  $J$  defined on the whole Banach space  $\ell_2(\Lambda, \mathbb{R}^M) \times \ell_{\infty, \rho^{-1}}(\Lambda)$  rather than just for positive  $v_\lambda$ 's (which is needed to use subdifferentials) we simply extend  $J(u, v)$  by

$$J(u, v) = \infty \quad \text{if } v_\lambda < 0 \text{ for some } \lambda \in \Lambda$$

as usual. This extension preserves convexity and does not change the minimizer.

Recall that  $J$  can be written as  $J(u, v) = \mathcal{T}(u) + \Phi^{(q)}(u, v)$ , see (6). Since both  $\mathcal{T}$  and  $\Phi^{(q)}$  are convex we have, see e.g. [24, Proposition 5.6],

$$\partial J(u, v) = \partial \mathcal{T}(u) \times \{0\} + \partial \Phi^{(q)}(u, v). \quad (13)$$

Concerning the subdifferential of  $\mathcal{T}$  we have the following result.

**Lemma 3.2.** *The subdifferential of  $\mathcal{T}$  at  $u \in \ell_2(\Lambda, \mathbb{R}^M)$  consists of one element,*

$$\partial \mathcal{T}(u) = \{2T^*(Tu - g)\}.$$

*Proof.* Since  $\mathcal{T}$  is convex and Gateaux-differentiable, by Proposition 5.3 [24] we have  $\partial \mathcal{T}(u) = \{\mathcal{T}'(u)\}$ , where its Gateaux-derivative is characterized by  $\langle \mathcal{T}'(u), z \rangle = \lim_{h \rightarrow 0^+} \frac{\mathcal{T}(u+hz) - \mathcal{T}(u)}{h}$  for all  $z \in \ell_2(\Lambda, \mathbb{R}^M)$ . It is straightforward to check that the Gateaux derivative of a functional of the type  $u \rightarrow \|Tu - g\|^2$  (with linear  $T$ ) at  $u$  applied on  $z$  is given by  $2\langle Tu - g, Tz \rangle = 2\langle T^*(Tu - g), z \rangle$ . This proves the claim.  $\square$

Let us now consider the subdifferential of  $\partial \Phi^{(q)}(u, v)$ . Recall its domain  $\ell_2(\Lambda, \mathbb{R}^M) \times \ell_{\infty, \rho^{-1}}(\Lambda)$ . Since the dual of  $\ell_{\infty, \rho^{-1}}$  is a bit inconvenient to handle we restrict the subdifferential to the predual  $\ell_{1, \rho}$ . This will be enough for our purposes. Moreover, recall that  $\Phi^{(q)}$  decouples into a sum of functionals  $\Phi_\lambda^{(q)}$  depending only  $(u_\lambda, v_\lambda)$ , see (7). It is straightforward to show the following lemma.

**Lemma 3.3.** *The subdifferential of  $\Phi^{(q)}$  at a point  $(u, v) \in \ell_2(\Lambda, \mathbb{R}^M) \times \ell_{\infty, \rho^{-1}}(\Lambda)$  with  $\Phi^{(q)}(u, v) < \infty$  satisfies*

$$\begin{aligned} D\Phi^{(q)}(u, v) &:= \partial \Phi^{(q)}(u, v) \cap (\ell_2(\Lambda, \mathbb{R}^M) \times \ell_{1, \rho}(\Lambda)) \\ &= \{(\xi, \eta) \in \ell_2(\Lambda, \mathbb{R}^M) \times \ell_{1, \rho}(\Lambda) : (\xi_\lambda, \eta_\lambda) \in \partial \Phi_\lambda^{(q)}(u_\lambda, v_\lambda) \text{ for all } \lambda \in \Lambda\}. \end{aligned}$$

We are left with investigating the subdifferential of the functional  $\Phi_\lambda^{(q)}$  defined in (8). Similarly as  $J$  we extend it to  $\mathbb{R}^M \times \mathbb{R}$  by  $\Phi_\lambda^{(q)}(x, y) = \infty$  for  $y < 0$ .

**Lemma 3.4.** *Let  $1 \leq q \leq \infty$ . Assume that  $\Phi_\lambda^{(q)}$  is convex (see also Proposition 2.1). Then for  $(x, y) \in \mathbb{R}^M \times \mathbb{R}_+$  we have*

$$\partial\Phi_\lambda^{(q)}(x, y) = \{(\xi, \eta) \in \mathbb{R}^M \times \mathbb{R} : \xi \in y\partial\|\cdot\|_q(x) + 2\omega_\lambda x, \eta \in \|x\|_q \partial s^+(y) + 2\theta_\lambda(y - \rho_\lambda)\}. \quad (14)$$

where  $s^+(y) := y$  for  $y \geq 0$  and  $s^+(y) = \infty$  for  $y < 0$ . In particular,  $\partial s^+(y) = \{1\}$  for  $y > 0$  and  $\partial s^+(0) = (-\infty, 1]$ .

*Remark:* We recall that the subdifferential of the  $q$ -norm on  $\mathbb{R}^M$  is given as follows. If  $1 < q < \infty$  then

$$\partial\|\cdot\|_q(x) = \begin{cases} B^{q'}(1) & \text{if } x = 0, \\ \left\{ \left( \frac{|x_\ell|^{q-1} \text{sign}(x_\ell)}{\|x\|_q^{1-1/q}} \right)_{\ell=1}^M \right\} & \text{otherwise,} \end{cases}$$

where  $B^{q'}(1)$  denotes the ball of radius 1 in the dual norm, i.e., in  $\ell_{q'}$  with  $1/q + 1/q' = 1$ .

If  $q = 1$  then

$$\partial\|\cdot\|_1(x) = \{\xi \in \mathbb{R}^M : \xi_\ell \in \partial|\cdot|(x_\ell), \ell = 1, \dots, M\} \quad (15)$$

where  $\partial|\cdot|(z) = \{\text{sign}(z)\}$  if  $z \neq 0$  and  $\partial|\cdot|(0) = [-1, 1]$ .

If  $q = \infty$  then

$$\partial\|\cdot\|_\infty(x) = \begin{cases} B^1(1) & \text{if } x = 0, \\ \text{conv}\{(\text{sign}(x_\ell)e_\ell : |x_\ell| = \|x\|_\infty)\} & \text{otherwise,} \end{cases} \quad (16)$$

where  $\text{conv } A$  denotes the convex hull of a set  $A$  and  $e_\ell$  the  $\ell$ -th canonical unit vector in  $\mathbb{R}^M$ .

*Proof.* Recall that

$$\Phi_\lambda^{(q)}(x, y) = s^+(y)\|x\|_q + \omega_\lambda\|x\|_2^2 + \theta_\lambda(\rho_\lambda - y)^2.$$

Let  $y \geq 0$  so that  $\Phi_\lambda^{(q)}(x, y)$  is finite. The subdifferential  $\partial(\Phi_\lambda^{(q)})_x(x, y)$  of  $\Phi_\lambda^{(q)}(x, y)$  considered as a function of  $x$  alone (i.e. for fixed  $y$ ) is clearly given by

$$\partial(\Phi_\lambda^{(q)})_x(x, y) = y\partial\|\cdot\|_q(x) + 2\omega_\lambda x \quad (17)$$

while keeping  $y$  fixed gives

$$\partial(\Phi_\lambda^{(q)})_y(x, y) = \partial s^+(y)\|x\|_q + 2\theta_\lambda(y - \rho_\lambda).$$

This shows the inclusion ' $\subset$ ' in (14). Moreover, for all the points  $(x, y) \in \mathbb{R}^M \times \mathbb{R}_+$  where  $\Phi_\lambda^{(q)}$  is differentiable we even have equality in (14) since  $\Phi_\lambda^{(q)}$  is convex and, thus, all the subdifferentials appearing consist of precisely one point, i.e., the usual gradient.

Let  $1 < q < \infty$ . Then for  $x \neq 0$ ,  $y > 0$  the differentiability assumption is clearly satisfied. For the other cases  $x = 0$  or  $y = 0$  we note that by convexity of  $\Phi_\lambda^{(q)}$  we have (see [37, Corollary 10.11])

$$\partial(\Phi_\lambda^{(q)})_x(x, y) = \{\xi : \exists \eta \text{ such that } (\xi, \eta) \in \partial\Phi_\lambda^{(q)}(x, y)\} \quad (18)$$

and the corresponding relation for  $\partial(\Phi_\lambda^{(q)})_y(x, y)$ . Now, if  $y > 0$  then  $\Phi_\lambda^{(q)}(x, y)$  is differentiable with respect to  $y$  and thus,  $\eta$  in the right hand side of (18) is unique, indeed  $\eta = \eta_0 := \frac{\partial}{\partial y}\Phi_\lambda^{(q)}(x, y)$ . We conclude that for  $y > 0$

$$\partial(\Phi_\lambda^{(q)})(x, y) = \{(\xi, \eta_0), \xi \in \partial(\Phi_\lambda^{(q)})_x(x, y)\}$$

In particular this holds for  $x = 0$ , even for general  $1 \leq q \leq \infty$ . The same argument applies for the case  $y = 0$  and  $x \neq 0$  (and  $1 < q < \infty$ ), which shows (14) in these cases. Now let  $x = 0$  and  $y = 0$ . Then the right hand side of (14) contains precisely one point, i.e.,  $(\xi, \eta) = (0, -2\theta_\lambda\rho_\lambda)$ . Since the subdifferential  $\Phi_\lambda^{(q)}(0, 0)$  contains at least one point by convexity, it must coincide with  $(\xi, \eta)$  by the trivial inclusion ' $\subset$ '. (It is easy to check also directly that  $(0, -2\theta_\lambda\rho_\lambda) \in \Phi_\lambda^{(q)}(0, 0)$ ). Note that this argument applies also for  $q = 1, \infty$ .

It remains to treat the cases  $q = 1, \infty$  with  $x \neq 0$  and arbitrary  $y \geq 0$ . Let us start with  $q = 1$ . In the proof of Proposition 2.1 it was noted that

$$\Phi_\lambda^{(1)}(x, y) = \sum_{\ell=1}^M F_\lambda^{(1)}(x_\ell, y)$$

with  $F_\lambda^{(1)} : \mathbb{R}^2 \rightarrow \mathbb{R}$  defined in (9). The subdifferential of  $F_\lambda$  can be obtained in the same way as above (expressing e.g. formally the modulus as a 2-norm on  $\mathbb{R}^1$ ). For  $(z, y) \in \mathbb{R} \times \mathbb{R}_+$  this yields

$$\partial F_\lambda^{(1)}(z, y) = \{(\tau, \eta) : \tau \in y\partial|\cdot|(z) + 2\omega_\lambda z, \eta \in |z|\partial s^+(y) + 2M^{-1}\theta_\lambda(y - \rho_\lambda)\}.$$

By convexity we have

$$\partial\Phi_\lambda^{(1)}(x, y) = \sum_{\ell=1}^M \left\{ (e_\ell z_\ell, \eta) : (z_\ell, \eta) \in \partial F_\lambda^{(1)}(x_\ell, y) \right\}$$

where  $e_\ell$  denotes the  $\ell$ -th unit vector in  $\mathbb{R}^M$ . By the explicit form of the subdifferential of the  $\ell_1$ -norm (15) this gives (14) for  $q = 1$ .

Finally, let  $q = \infty$ . Similarly as in the proof of Proposition 2.1 we write

$$\Phi_\lambda^{(\infty)}(x, y) = \max_{\ell=1, \dots, M} F_\ell(x, y)$$

with

$$F_\ell(x, y) = y|x_\ell| + \omega_\lambda\|x\|_2^2 + \theta_\lambda(\rho_\lambda - y)^2.$$

If  $x_\ell \neq 0$  then  $F_\ell(x, y)$  is differentiable with respect to  $x$  and

$$\partial F_\ell(x, y) = \{(\xi, \eta) : \xi = y \operatorname{sign}(x_\ell)e_\ell + 2\omega_\lambda x, \eta \in \partial s^+(y)|x_\ell| + 2\theta_\lambda(y - \rho_\lambda)\},$$

where  $e_\ell$  denotes the  $\ell$ -th canonical unit vector in  $\mathbb{R}^M$ . This even holds for  $y = 0$  by an analogous argument as above, see (18). The subdifferential of  $\Phi_\lambda^{(\infty)}(x, y)$  for  $x \neq 0$  is then given by (see e.g. [37, Exercise 8.31])

$$\partial\Phi_\lambda^{(\infty)}(x, y) = \text{conv}\{\partial F_\ell(x, y) : F_\ell(x, y) = \max_{m=1, \dots, M} F_m(x, y)\}.$$

Since  $x \neq 0$  we have  $x_\ell \neq 0$  if  $|x_\ell| = \|x\|_\infty$  and the latter is the case iff  $F_\ell(x, y) = \max_m F_m(x, y)$ . Thus, we obtain

$$\begin{aligned} & \partial\Phi_\lambda^{(\infty)}(x, y) \\ &= \text{conv} \bigcup_{\ell: |x_\ell| = \|x\|_\infty} \{(\xi, \eta) : \xi = y \text{sign}(x_\ell)e_\ell + 2\omega_\lambda x, \eta \in \partial s^+(y)|x_\ell| + 2\theta_\lambda(y - \rho_\lambda)\} \\ &= \{(\xi, \eta) : \xi \in \text{conv}\{y \text{sign}(x_\ell)e_\ell, |x_\ell| = \|x\|_\infty\}, \eta \in \|x\|_\infty \partial s^+(y)\} + (2\omega_\lambda x, 2\theta_\lambda(y - \rho_\lambda)). \end{aligned}$$

By the characterization of the subdifferential of the  $\infty$ -norm in (16) we obtain the claimed equality in (14) for  $q = \infty$  and  $x \neq 0$ . This finishes the proof.  $\square$

Combining the previous lemmas we obtain the following result.

**Proposition 3.5.** *Let  $1 \leq q \leq \infty$ . Assume that  $\Phi^{(q)}$  is convex and let  $(u, v) \in \ell_2(\Lambda, \mathbb{R}^M) \times \ell_{\infty, \rho^{-1}}(\Lambda)$  such that  $\Phi^{(q)}(u, v) < \infty$ . Then we have*

$$\begin{aligned} D\Phi^{(q)}(u, v) &= \{(\xi, \eta) \in \ell_2(\Lambda, \mathbb{R}^M) \times \ell_{1, \rho}(\Lambda), \xi_\lambda \in v_\lambda \partial \|\cdot\|_q(u_\lambda) + 2\omega_\lambda u_\lambda, \\ &\quad \eta_\lambda \in \|u_\lambda\|_q \partial s^+(v_\lambda) + 2\theta_\lambda(v_\lambda - \rho_\lambda), \lambda \in \Lambda\} \\ &\subset \partial\Phi^{(q)}(u, v) \end{aligned} \tag{19}$$

and

$$DJ(u, v) = \partial J(u, v) \cap (\ell_2(\Lambda, \mathbb{R}^M) \times \ell_{1, \rho}(\Lambda)) = (2T^*T(u - g), 0) + D\Phi_\lambda^{(q)}(u, v) \subset \partial J(u, v).$$

### 3.2 Weak convergence of the double-minimization

Before we actually start proving the weak convergence of the algorithm in (11) we recall the following definition [37].

**Definition 1.** Let  $V$  be a topological space and  $\mathcal{A} = (A_n)_{n \in \mathbb{N}}$  a sequence of subsets of  $V$ . The subset  $A \subseteq V$  is called the *limit of the sequence*  $\mathcal{A}$ , and we write  $A = \lim_n A_n$ , if

$$A = \{a \in V : \exists a_n \in A_n, a = \lim_n a_n\}.$$

The following observation will be useful for us, see e.g. [37, Proposition 8.7].

**Lemma 3.6.** *Assume that  $\Gamma$  is a convex function on  $\mathbb{R}^M$  and  $(x_n) \subset \mathbb{R}^M$  a convergent sequence with limit  $x$  such that  $\Gamma(x_n), \Gamma(x) < \infty$ . Then the subdifferentials satisfy*

$$\lim_n \partial\Gamma(x_n) \subseteq \partial\Gamma(x).$$

*In other words, the subdifferential  $\partial\Gamma$  of a convex function is an outer semicontinuous set-valued function.*

In the following we agree on the convention that the upper index  $n$  at  $u^{(n)} \in \ell_2(\Lambda, \mathbb{R}^M)$  always denotes the  $n$ -th iterate and  $u_\lambda^{(n)} \in \mathbb{R}^M$  denotes the (vector-valued) entry at  $\lambda$  of the  $n$ -th iterate. In the following proof we will never refer to the  $\ell$ -th component of the  $M$ -dimensional vector  $u_\lambda^{(n)}$ , so hopefully no confusion can arise. Also, we denote by  $(DJ(u, v))_\lambda$  the restriction of  $DJ(u, v) \subset \ell_2(\Lambda, \mathbb{R}^M) \times \ell_{1,\rho}(\Lambda)$  to the index  $\lambda$ . By the previous section it holds

$$(DJ(u, v))_\lambda = (2T^*T(u - g))_\lambda, 0) + \partial\Phi_\lambda^{(q)}(u_\lambda, v_\lambda). \quad (20)$$

Now the proof is developed as follows. First, we recall that  $(u^*, v^*) = \arg \min J(u, v)$  if and only if  $0 \in \partial J(u^*, v^*)$ . Next, we show that there exist weakly convergent subsequences of  $(u^{(n)}, v^{(n)})$  (again denoted by  $(u^{(n)}, v^{(n)})$ ) which converge to  $(u^{(\infty)}, v^{(\infty)})$  and that

$$0 \in \lim_n DJ(u^{(n)}, v^{(n)}) \subseteq \partial J(u^{(\infty)}, v^{(\infty)}). \quad (21)$$

Due to the strict convexity of  $J$  we conclude that  $(u^{(\infty)}, v^{(\infty)}) = (u^*, v^*)$ . Now, let us detail the argument.

By definition of  $u^{(n)}$  and  $v^{(n)}$  we have

$$\begin{aligned} & J(u^{(n)}, v^{(n)}) - J(u^{(n+1)}, v^{(n+1)}) \\ &= J(u^{(n)}, v^{(n)}) - J(u^{(n+1)}, v^{(n)}) + J(u^{(n+1)}, v^{(n)}) - J(u^{(n+1)}, v^{(n+1)}) \geq 0. \end{aligned}$$

Thus,  $(J(u^{(n)}, v^{(n)}))_n$  is a nonincreasing sequence, and since  $J \geq 0$  this implies that  $(J(u^{(n)}, v^{(n)}))_n$  converges. Moreover,

$$J(u^{(0)}, v^{(0)}) \geq J(u^{(n)}, v^{(n)}) \geq \sum_{\lambda \in \Lambda} \omega_\lambda \|u_\lambda^{(n)}\|_2^2.$$

Therefore,  $(u^{(n)})_n$  is uniformly bounded in  $\ell_{2,\omega^{1/2}}(\Lambda, \mathbb{R}^M)$  and thus, there exists a subsequence  $(u^{(n_k)})_k$  that converges to  $u^{(\infty)} \in \ell_{2,\omega^{1/2}}(\Lambda, \mathbb{R}^M)$  weakly in both  $\ell_{2,\omega^{1/2}}(\Lambda, \mathbb{R}^M)$  and  $\ell_2(\Lambda, \mathbb{R}^M)$ , due to our assumption  $\omega_\lambda \geq \gamma > 0$  for all  $\lambda \in \Lambda$ . For simplicity, let us denote again  $u^{(n_k)} = u^{(n)}$ .

First of all, observe that weak convergence implies componentwise convergence, so that  $u_\lambda^{(n)} \rightarrow u_\lambda^{(\infty)}$  and  $[T^*Tu^{(n)}]_\lambda \rightarrow [T^*Tu^{(\infty)}]_\lambda$  for all  $\lambda \in \Lambda$ . By the explicit formula (12) for  $v_\lambda^{(n)}$  this implies that  $v^{(n)}$  converges pointwise to the limit

$$v_\lambda^{(\infty)} := \lim_n v_\lambda^{(n)} = \begin{cases} \rho_\lambda - \frac{1}{2\theta_\lambda} \|u^{(\infty)}_\lambda\|_q & \text{if } \|u^{(\infty)}_\lambda\|_q < 2\theta_\lambda \rho_\lambda, \\ 0 & \text{otherwise.} \end{cases} \quad (22)$$

By definition of  $u^{(n)}$  in (11) we have  $0 \in \partial J_u(u, v^{(n)})$  (where  $\partial J_u(u, v)$  denotes the subdifferential of  $J$  considered as a functional of  $u$  only). This means that

$$0 \in \left[ 2T^*(Tu^{(n)} - g) \right]_\lambda + v_\lambda^{(n-1)} \partial \|\cdot\|_q(u_\lambda^{(n)}) + 2\omega_\lambda u_\lambda^{(n)} \quad \text{for all } \lambda \in \Lambda,$$

see also Lemma 3.2 and (17), in other words

$$0 = \left[ 2T^*(Tu^{(n)} - g) \right]_\lambda + v_\lambda^{(n-1)} \zeta_\lambda^{(n)} + 2\omega_\lambda u_\lambda^{(n)}, \quad (23)$$

for a suitable  $\zeta_\lambda^{(n)} \in \partial \|\cdot\|_q(u_\lambda^{(n)})$ . Now, let  $(\xi^{(n)}, \eta^{(n)}) \in DJ(u^{(n)}, v^{(n)})$ . By definition of  $DJ$  and by (23) we have

$$\xi_\lambda^{(n)} \in [2T^*(Tu^{(n)} - g)]_\lambda + v_\lambda^{(n)} \partial \|\cdot\|_q(u_\lambda^{(n)}) + 2\omega_\lambda u_\lambda^{(n)} = v_\lambda^{(n)} \partial \|\cdot\|_q(u_\lambda^{(n)}) - v_\lambda^{(n-1)} \zeta_\lambda^{(n)},$$

for a suitable  $\zeta_\lambda^{(n)} \in \partial \|\cdot\|_q(u_\lambda^{(n)})$ . Since  $v_\lambda^{(n)}$  converges it is possible to choose the sequence  $\xi^{(n)}$  such that  $\lim_{n \rightarrow \infty} \xi_\lambda^{(n)} = 0$  for all  $\lambda \in \Lambda$ . From (22) it is straightforward to check that

$$0 \in \partial s^+(v_\lambda^{(\infty)}) \|u_\lambda^{(\infty)}\|_q + 2\theta_\lambda (v_\lambda^{(\infty)} - \rho_\lambda) \quad \text{for all } \lambda \in \Lambda, \quad (24)$$

and similarly

$$0 \in \partial s^+(v_\lambda^{(n)}) \|u_\lambda^{(n)}\|_q + 2\theta_\lambda (v_\lambda^{(n)} - \rho_\lambda)$$

We can choose  $\eta^{(n)} = 0$  so that  $\lim_n \eta_\lambda^{(n)} = 0$  for all  $\lambda \in \Lambda$ . Altogether we conclude that  $0 \in \lim_n (DJ(u^{(n)}, v^{(n)}))_\lambda$  for all  $\lambda \in \Lambda$ . By continuity of  $T$  and Lemma 3.6 we conclude

$$\begin{aligned} 0 &\in \lim_n \left[ (2(T^*T(u^{(n)} - g))_\lambda, 0) + \partial \Phi_\lambda^{(q)}(u_\lambda^{(n)}, v_\lambda^{(n)}) \right] \\ &\subset (2T^*T(u^{(\infty)} - g)_\lambda, 0) + \partial \Phi_\lambda^{(q)}(u_\lambda^{(\infty)}, v_\lambda^{(\infty)}) = DJ(u^{(\infty)}, v^{(\infty)})_\lambda \end{aligned}$$

for all  $\lambda \in \Lambda$ . It follows that  $0 \in DJ(u^{(\infty)}, v^{(\infty)}) \subset \partial J(u^{(\infty)}, v^{(\infty)})$ , the latter inclusion by Proposition (3.5). Hence, by strict convexity  $(u^*, v^*) = (u^{(\infty)}, v^{(\infty)})$ . With this we have shown the weak convergence of the sequence  $u^{(n)}$  to  $u^*$ .

To establish the strong convergence we need to develop a more detailed analysis of the minimization of  $J$  with respect to  $u$ . Next section is devoted to this end, and it will allow us to use some further tools for the full proof of Theorem 3.1 in Subsection 5.3.

## 4 An Iterative Thresholding Algorithm for the Minimization with Respect to $u$

One step of the minimization algorithm in the previous section consists in minimizing  $J(u, v) = J_{\theta, \rho, \omega}^{(q)}(u, v)$  for some fixed  $v$ . Moreover, keeping  $v$  fixed is also interesting for its own – in particular, if one is interested in minimizing the functional  $K = K_v^{(q)}$  defined in (26). Indeed, for  $\omega = 0$  and  $\rho = v$  we have  $J_{\theta, v, 0}^{(q)}(u, v) = K_v^{(q)}(u)$ . As we will describe in the following this minimization task can be performed by a thresholded Landweber algorithm similar to the one analyzed by Daubechies et al. in [17].

With  $v$  fixed our task is equivalent to minimizing

$$K(u) = K_{v, \omega}^{(q)} := \|Tu - g\|_{\mathcal{H}}^2 + \Psi(u) \quad (25)$$

with respect to  $u \in \ell_2(\Lambda, \mathbb{R}^M)$  where

$$\Psi(u) := \Psi_{v, \omega}^{(q)}(u) := \sum_{\lambda \in \Lambda} v_\lambda \|u_\lambda\|_q + \sum_{\lambda \in \Lambda} \omega_\lambda \|u_\lambda\|_2^2. \quad (26)$$



We assume that  $T$  is non-expansive, i.e.,  $\|T\| < 1$ , which can always be achieved by rescaling. Also we suppose that  $K$  is strictly convex. This is ensured if e.g. the kernel of  $T$  is trivial or  $\omega_\lambda > 0$  for all  $\lambda \geq 0$ .

We define a surrogate functional by

$$K^s(u, a) := K(u) - \|Tu - Ta\|_{\mathcal{H}}^2 + \|u - a\|_2^2 = \|Tu - g\|_{\mathcal{H}}^2 + \Psi(u) - \|Tu - Ta\|_{\mathcal{H}}^2 + \|u - a\|_2^2.$$

Since  $\|T\| < 1$  also  $K^s$  is convex, see [17] for a rigorous argument. Now starting with some  $u^{(0)} \in \ell_2(\Lambda, \mathbb{R}^M)$  we define a sequence  $u^{(m)}$  by

$$u^{(m+1)} = \arg \min_{u \in \ell_2(\Lambda, \mathbb{R}^M)} K^s(u, u^{(m)})$$

The minimizer of  $K^s(u, a)$  (for fixed  $a$ ) can be determined explicitly as follows. First, we claim that

$$\arg \min_u K^s(u, a) = U_\Psi(a + T^*(g - Ta)),$$

where the ‘‘thresholding’’ operator  $U_\Psi$  is defined as

$$U_\Psi(u) := \arg \min_{z \in \ell_2(\Lambda, \mathbb{R}^M)} \|u - z\|_2^2 + \Psi(z). \quad (27)$$

Indeed, a direct calculation shows that

$$\begin{aligned} K^s(u, a) &= \|Tu - g\|_{\mathcal{H}}^2 - \|Tu - Ta\|_{\mathcal{H}}^2 + \|u - a\|_2^2 + \Psi(u) \\ &= \|(a + T^*(g - Ta)) - u\|_2^2 + \Psi(u) - \|a + T^*(g - Ta)\|_2^2 + \|g\|_{\mathcal{H}}^2 - \|Ta\|_{\mathcal{H}}^2 + \|a\|_2^2. \end{aligned}$$

Since the last terms (after  $\Psi(u)$ ) do not depend on  $u$  they can be discarded when minimizing with respect to  $u$ , and the above claim follows. (The same argument works also for general ‘sparseness measures’  $\Psi$ ). Thus, the iterative algorithm reads

$$u^{(m+1)} = U_\Psi(u^{(m)} + T^*(g - Tu^{(m)})). \quad (28)$$

In the following we give more details about  $U_\Psi$  and analyze the convergence of this algorithm.

#### 4.1 The thresholding operator

Let us derive more information about  $U_\Psi$  for our specific  $\Psi = \Psi_{v, \omega}$  in (26). We have the following lemma.

**Lemma 4.1.** *Let  $1 \leq q \leq \infty$ . It holds*

$$(U_{v, \omega}^{(q)}(u))_\lambda := (U_{\Psi_{v, \omega}^{(q)}}(u))_\lambda = (1 + \omega_\lambda)^{-1} S_{v_\lambda}^{(q)}(u_\lambda),$$

where

$$S_v^{(q)}(x) = \arg \min_{z \in \mathbb{R}^M} \|z - x\|_2^2 + v \|z\|_q, \quad x \in \mathbb{R}^M. \quad (29)$$

Furthermore,  $S_v^{(q)}$  is given by

$$S_v^{(q)}(x) = x - P_{v/2}^q(x), \quad (30)$$

where  $P_{v/2}^{q'}$  denotes the orthogonal projection onto the norm ball of radius  $v/2$  with respect to the dual norm of  $\|\cdot\|_q$ , i.e., the  $\|\cdot\|_{q'}$ -norm with  $q'$  denoting the dual index,  $1/q + 1/q' = 1$ . (The analogous result holds also if the norm  $\|\cdot\|_q$  is replaced by an arbitrary norm on  $\mathbb{R}^M$ ).

*Proof.* For  $\Psi_{v,\omega}$  the minimizing problem defining  $U_\Psi = U_{v,\omega}^{(q)}$  decouples with respect to  $\lambda \in \Lambda$ . Thus, we have

$$(U_{v,\omega}^{(q)}(x))_\lambda = \arg \min_{z \in \mathbb{R}^M} \|x_\lambda - z\|_2^2 + \omega_\lambda \|z\|_2^2 + v_\lambda \|z\|_q.$$

If  $z$  minimizes the latter term then necessarily  $0 \in 2(1 + \omega_\lambda)z - 2x + v_\lambda \partial \|\cdot\|_q(z)$  where  $\partial \|\cdot\|_q$  denotes the subdifferential of the  $q$ -norm. In other words,

$$(1 + \omega_\lambda)z - x \in -\frac{v_\lambda}{2} \partial \|\cdot\|_q(z).$$

Since  $\|\cdot\|_q$  is 1-homogeneous we have  $\partial \|\cdot\|_q(z) = \partial \|\cdot\|_q((1 + \omega_\lambda)z)$ . Setting  $y = (1 + \omega_\lambda)z$  gives  $y - x \in -\frac{v_\lambda}{2} \partial \|\cdot\|_q(y)$ , which is the above relation for  $\omega_\lambda = 0$ . From this we deduce the first claim.

Let us show the second claim, i.e., the explicit form of the operator  $S_v^{(q)}$ . We already know that if  $z$  minimizes the left hand side of (29) then  $x - z \in \partial \frac{v}{2} \|z\|_q$ . Let  $\psi(z) = \frac{v}{2} \|z\|_q$  and  $\psi^*$  be its Fenchel conjugate function defined by  $\psi^*(y) = \sup_x (\langle x, y \rangle - \psi(x))$ . It is well-known [4, p. 93] that

$$\psi^*(y) = \chi_{B^{q'}(v/2)}(y) := \begin{cases} 0 & \text{if } \|y\|_{q'} \leq v/2 \\ \infty & \text{otherwise} \end{cases}$$

Here  $B^{q'}(v/2)$  denotes the norm ball of radius  $v/2$  with respect to the dual norm of  $\|\cdot\|_q$ . It is a standard result, see e.g. [37, Proposition 11.3], [24, Corollary 5.2], that  $w \in \partial \psi(y)$  if and only if  $y \in \partial \psi^*(w)$  yielding  $z \in \partial \psi^*(x - z)$  in our case, and hence,

$$x \in x - z + \partial \psi^*(x - z) = x - z + \partial \chi_{B^{q'}(v/2)}(x - z).$$

Now if  $y \in w + \partial \chi_{B^{q'}(v/2)}(w)$  then it is straightforward to see that  $w$  must be the orthogonal projection of  $y$  onto  $B^{q'}(v/2)$ , i.e.,  $w = \arg \min_{w' \in B^{q'}(v/2)} \|w' - y\|_2$ , see also [37, Example 10.2 and p. 20]. For our situation this means that  $x - z = P_{v/2}^{q'}(x)$ , i.e.,  $z = x - P_{v/2}^{q'}(x)$ . This shows the second claim.

Clearly, all arguments work also for a general norm rather than the  $q$ -norm.  $\square$

Let us give  $S_v^{(q)}$  explicitly for  $q = 1, 2, \infty$ .

**Lemma 4.2.** *Let  $x \in \mathbb{R}^M$  and  $v \geq 0$ .*

(a) *For  $q = 1$  we have  $S_v^{(1)}(x) = (s_v^{(1)}(x_\ell))_{\ell=1}^M$  where for  $y \in \mathbb{R}$*

$$s_v^{(1)}(y) = \begin{cases} 0 & \text{if } |y| \leq \frac{v}{2}, \\ \text{sign}(y)(|y| - \frac{v}{2}) & \text{otherwise.} \end{cases}$$

(b) For  $q = 2$  it holds

$$S_v^{(2)}(x) := \begin{cases} 0 & \text{if } \|x\|_2 \leq \frac{v}{2}, \\ \frac{(\|x\|_2 - v/2)}{\|x\|_2} x & \text{otherwise.} \end{cases}$$

(c) Let  $q = \infty$ . Order the entries of  $x$  by magnitude such that  $|x_{i_1}| \geq |x_{i_2}| \geq \dots \geq |x_{i_M}|$ .

1. If  $\|x\|_1 < v/2$  then  $S_v^{(\infty)}(x) = 0$ .
2. If  $\|x\|_1 > v/2$ , let  $n \in \{1, \dots, M\}$  be the largest index satisfying

$$|x_{i_n}| \geq \frac{1}{n-1} \left( \sum_{k=1}^{n-1} |x_{i_k}| - \frac{v}{2} \right). \quad (31)$$

Then

$$\begin{aligned} (S_v^{(\infty)}(x))_{i_j} &= \frac{\text{sign}(x_{i_j})}{n} \left( \sum_{k=1}^n |x_{i_k}| - \frac{v}{2} \right), \quad j = 1, \dots, n, \\ (S_v^{(\infty)}(x))_{i_j} &= x_{i_j}, \quad j = n+1, \dots, M. \end{aligned}$$

*Proof.* (b) The projection  $P_{v/2}^2(x)$  of  $x$  onto an  $\ell_2$  ball of radius  $v/2$  is clearly given by

$$P_{v/2}^2(x) = \begin{cases} x & \text{if } \|x\|_2 \leq v/2, \\ \frac{v/2}{\|x\|_2} x & \text{otherwise.} \end{cases}$$

Since by the previous lemma  $S_v^{(2)}(x) = x - P_{v/2}^2(x)$  this gives the assertion.

(a) Although this is well-known we give a simple argument. For  $q = 1$  the functional in (29) defining  $S^{(1)}$  decouples, i.e.,

$$S_v^{(1)}(x) = \arg \min_{z \in \mathbb{R}^M} \sum_{\ell=1}^M (|z_\ell - x_\ell|^2 + v|z_\ell|).$$

Thus,  $S_v^{(1)}(x)_\ell = \arg \min_{z_\ell \in \mathbb{R}} |z_\ell - x_\ell|^2 + v|z_\ell|$  for all  $\ell = 1, \dots, M$ . The latter can be interpreted as the problem for  $q = 2$  on  $\mathbb{R}^1$  and hence, the assertion follows from (b).

(c) If  $\|x\|_1 \leq v/2$  then  $P_{v/2}^1(x) = x$  and by the previous lemma  $S_v^{(\infty)}(x) = x - P_{v/2}^1(x) = 0$ . Now assume  $\|x\|_1 > v/2$ . Let  $z = S_v^{(\infty)}(x)$ . This is equivalent to 0 being contained in the subdifferential of the functional in (29) defining  $S_v^{(\infty)}$ . This means

$$2(z - x) \in -v\partial\|\cdot\|_\infty(z). \quad (32)$$

We recall that the subdifferential of the maximum norm is given by (16).

Now assume for the moment that the maximum norm of  $z$  is attained in  $z_{i_1}, \dots, z_{i_n}$ . We will later check whether this was really the case. Further, we assume for simplicity that all the entries  $x_{i_1}, \dots, x_{i_n}$  are positive. (The other cases can be carried through in the same way). Then certainly also the numbers  $z_{i_1}, \dots, z_{i_n}$  are positive because choosing them

with the opposite sign would certainly increase the functional defining  $S_v^{(\infty)}$ . Then by (16) we obtain  $2(z_{i_j} - x_{i_j}) = 0$  for the entries  $z_{i_j}$  not giving the maximum, i.e.,  $z_{i_j} = x_{i_j}, j = n + 1, \dots, M$ .

Moreover, if  $n = 1$  (i.e., the maximum norm of  $z$  is attained at only one entry) then  $2(z_{i_1} - x_{i_1}) = -v$ , in other words,  $z_{i_1} = x_{i_1} - v/2$ . Thus, the initial hypothesis that the maximum norm of  $z$  is attained only at  $z_{i_1}$  is true if and only if the second largest entry  $x_{i_2}$  satisfies  $|x_{i_2}| < |z_{i_1}| - v/2$ .

So if the latter inequality is not satisfied then the maximum norm of  $z$  is at least attained at two entries, i.e.,  $n \geq 2$ . In this case by (16) the entries  $z_{i_1} = z_{i_2} = \dots = z_{i_n} = t$  satisfy

$$\begin{aligned} 2t - 2x_{i_j} &= -va_j, \quad j = 1, \dots, n-1, \\ 2t - 2x_{i_n} &= -v \left( 1 - \sum_{k=1}^{n-1} a_k \right) \end{aligned}$$

for some numbers  $a_1, \dots, a_{n-1} \in [0, 1]$  satisfying  $\sum_j a_j \leq 1$ . This is a system of  $n$  linear equations in  $t$  and  $a_1, \dots, a_{n-1}$ . Writing it in matrix form we get

$$\begin{pmatrix} 1 & v/2 & 0 & 0 & \cdots & 0 \\ 1 & 0 & v/2 & 0 & \cdots & 0 \\ \vdots & \vdots & \vdots & \vdots & \ddots & \vdots \\ 1 & -v/2 & -v/2 & -v/2 & \cdots & -v/2 \end{pmatrix} \begin{pmatrix} t \\ a_1 \\ \vdots \\ a_{n-1} \end{pmatrix} = \begin{pmatrix} x_{i_1} \\ \vdots \\ x_{i_{n-1}} \\ x_{i_n} - v/2 \end{pmatrix}.$$

Denoting the matrix on the left hand side by  $B$ , a simple computation verifies that

$$B^{-1} = \frac{1}{n} \begin{pmatrix} 1 & 1 & 1 & \cdots & 1 \\ \frac{2(n-1)}{v} & -\frac{2}{v} & -\frac{2}{v} & \cdots & -\frac{2}{v} \\ -\frac{2}{v} & \frac{2(n-1)}{v} & -\frac{2}{v} & \cdots & -\frac{2}{v} \\ \vdots & \vdots & \ddots & \vdots & \vdots \\ -\frac{2}{v} & \cdots & -\frac{2}{v} & \frac{2(n-1)}{v} & -\frac{2}{v} \end{pmatrix}.$$

This gives

$$z_{i_1} = \dots = z_{i_n} = t = \frac{1}{n} \left( \sum_{j=1}^n x_{i_j} - v/2 \right)$$

and  $a_j = \frac{2}{nv} \left( v/2 + (n-1)x_{i_j} - \sum_{k \in \{1, \dots, n\} \setminus \{j\}} x_{i_k} \right)$ . Thus, all  $a_j$  are non-negative if for all  $j \in \{1, \dots, n-1\}$

$$x_{i_j} \geq \frac{1}{n-1} \left( \sum_{k \in \{1, \dots, n\} \setminus \{j\}} x_{i_k} - v/2 \right).$$

Moreover, a simple calculation gives  $\sum_{j=1}^{n-1} a_j = \frac{n-1}{n} + \frac{2}{nv} \left( \sum_{j=1}^{n-1} x_{i_j} - (n-1)x_{i_n} \right)$ . Thus, it holds  $1 - \sum_{j=1}^{n-1} a_j \geq 0$  if and only if

$$x_{i_n} \geq \frac{1}{n-1} \left( \sum_{j=1}^{n-1} x_{i_j} - v/2 \right).$$

Therefore, the initial assumption that the maximum norm of  $u$  is attained precisely at  $z_{i_1}, \dots, z_{i_n}$  can only be true if  $x_{i_1}, \dots, x_{i_n}$  are the largest entries of the vector  $x$  and

$$z_{i_{n+1}} = x_{i_{n+1}} < t = \frac{1}{n} \left( \sum_{j=1}^n x_{i_j} - v/2 \right),$$

i.e.,  $|x_{i_{n+1}}| < n^{-1}(\sum_{j=1}^n |x_{i_j}| - v/2)$ . Pasting all the pieces together shows the assertion of the lemma.  $\square$

## 4.2 Weak convergence

In the following we will prove that  $u^{(m)}$  converges weakly and strongly to the unique minimizer of  $K$ . We first establish the weak convergence. Following the proof of Proposition 3.11 in [17] one may extract essentially three conditions on a general sparsity measure  $\Psi$  such that weak convergence is ensured. Let us collect them in the following Proposition.

**Proposition 4.3.** *Assume  $K$  is given by (25) with a general sparsity measure  $\Psi$  and suppose  $K$  is strictly convex. Let  $U_\Psi$  be the associated 'thresholding operator' given by (27). Assume that the following conditions hold*

- (1)  $U_\Psi$  is non-expansive, i.e.  $\|U_\Psi(x) - U_\Psi(y)\|_2 \leq \|x - y\|_2$  for all  $x, y \in \ell_2(\Lambda, \mathbb{R}^M)$ .
- (2) It holds  $\|f\|_2 \leq H(\Psi(f))$  for all  $f \in \ell_2(\Lambda, \mathbb{R}^M)$  and some monotonically increasing function  $H$  on  $\mathbb{R}_+$ . (This ensures that a sequence  $f_n$  satisfying  $\Psi(f_n) \leq C$  is bounded in  $\ell_2(\Lambda, \mathbb{R}^M)$ ).
- (3) For all  $x, h \in \ell_2(\Lambda, \mathbb{R}^M)$  it holds

$$\Psi(U_\Psi(x) + h) - \Psi(U_\Psi(x)) + 2\langle h, U_\Psi(x) - x \rangle \geq 0.$$

Then the sequence  $u^{(m)}$  defined by (28) converges weakly to the minimizer of  $K$  independently of the choice of  $u^{(0)}$ .

*Proof.* First we claim that the condition in (1) implies that the surrogate functional  $K^s$  satisfies

$$K^s(u + h, a) - K^s(u, a) \geq \|h\|_2^2 \tag{33}$$

for  $u = \arg \min_{u'} K^s(u', a) = U_\Psi(a - T^*(g - Ta))$ . Indeed, set  $x := a - T^*(g - Ta)$ , i.e.,  $u = U_\Psi(x)$ . Then an elementary calculation yields

$$\begin{aligned} K^s(u + h, a) - K^s(u) &= \|T(u + h) - g\|_2^2 + \Psi(u + h) - \|T(u + h) - Ta\|_2^2 + \|u + h - a\|_2^2 \\ &\quad - \|Tu - g\|_2^2 - \Psi(u) + \|Tu - Ta\|_2^2 - \|u - a\|_2^2 \\ &= 2\langle h, u - a - T^*(g - Ta) \rangle + \Psi(u + h) - \Psi(u) + \|h\|_2^2 \\ &= 2\langle h, U_\Psi(x) - x \rangle + \Psi(U_\Psi(x) + h) - \Psi(U_\Psi(x)) + \|h\|_2^2 \geq \|h\|_2^2. \end{aligned}$$

The relation in (1) was used in the last inequality.

Now with (33) and properties (2) and (3) one can easily justify that the proofs of the analogues of Theorem 3.2 until Proposition 3.11 in [17] go through completely in the same way, which finally leads to the statement of this proposition.  $\square$

Let us now show that for our specific choice of  $\Psi = \Psi_{v,\omega}^{(q)}$  properties (1) - (3) in the previous Proposition hold, and thus,  $u^{(n)}$  converges weakly to a minimizer of  $K$ .

**Lemma 4.4.**  $U_{v,\omega}^{(q)} = U_{\Psi_{v,\omega}^{(q)}}$  is non-expansive.

*Proof.* Clearly, the map  $x \mapsto (1 + \omega_\lambda)^{-1}x$  is non-expansive. By (30) we have  $S_v^{(q)} = I - P_{v/2}^{q'}$ . Since  $P_{v/2}^{q'}$  is an orthogonal projection onto a convex set also  $S_v^{(q)}$  is non-expansive, see e.g. [39]. Hence,  $U_{v,\omega}^{(q)}$  is non-expansive since on each component  $x_\lambda$ ,  $\lambda \in \Lambda$ , it is a composition of non-expansive operators.  $\square$

**Lemma 4.5.** If  $(v_\lambda)$  or  $(\omega_\lambda)$  are bounded away from 0 then condition (2) in Proposition 4.3 holds.

*Proof.* This follows by a standard argument.  $\square$

If we consider the problem of minimizing  $J(u, v)$  jointly over  $u$  and  $v$  then we certainly cannot assume that  $v$  is bounded away from 0, but in this case we require that  $\omega_\lambda$  is bounded away from 0. (By Proposition 2.1 this is needed anyway to ensure that  $J(u, v)$  is jointly convex in  $u$  and  $v$ ). In the case where we only minimize  $J(u, v)$  with respect to  $u$  (i.e., when minimizing  $\Psi(u)$  defined in (26)) we may take  $\omega_\lambda$  arbitrary (and even  $\omega_\lambda = 0$ ) but then we have to require a lower bound on  $v_\lambda$ .

Now consider the third condition in the Proposition. The next lemma shows that it suffices to prove it for  $S_v^{(q)}$ , i.e., for  $\omega_\lambda = 0$ .

**Lemma 4.6.** Assume that for all  $x, h \in \mathbb{R}^M$  it holds

$$v(\|S_v^{(q)}(x) + h\|_q - \|S_v^{(q)}(x)\|_q) + 2\langle h, S_v^{(q)}(x) - x \rangle \geq 0.$$

Then condition (3) in Proposition 4.3 is satisfied.

*Proof.* By definition of  $\Psi_{v,\omega}^{(q)}$  we need to show that for  $\omega, v \geq 0$  and all  $x, h \in \mathbb{R}^M$

$$\begin{aligned} & v(\|(1 + \omega)^{-1}S_v^{(q)}(x) + h\|_q - \|(1 + \omega)^{-1}S_v^{(q)}(x)\|_q) \\ & + \omega(\|(1 + \omega)^{-1}S_v^{(q)}(x) + h\|_2^2 - \|(1 + \omega)^{-1}S_v^{(q)}(x)\|_2^2) + 2\langle h, (1 + \omega)^{-1}S_v^{(q)}(x) - x \rangle \geq 0. \end{aligned}$$

Setting  $h' = (1 + \omega)h$  we obtain for the left hand side of this inequality

$$\begin{aligned} & (1 + \omega)^{-1}v \left( \|S_v^{(q)}(x) + h'\|_q - \|S_v^{(q)}(x)\|_q \right) \\ & + (1 + \omega)^{-2}\omega \left( \|S_v^{(q)}(x) + h'\|_2^2 - \|S_v^{(q)}(x)\|_2^2 \right) + 2(1 + \omega)^{-2}\langle h', S_v^{(q)}(x) - x \rangle \\ & = (1 + \omega)^{-1} \left[ v(\|S_v^{(q)}(x) + h'\|_q - \|S_v^{(q)}(x)\|_q) + 2\langle h', S_v^{(q)}(x) - x \rangle \right] \\ & + (1 + \omega)^{-2}\omega \left[ \|S_v^{(q)}(x) + h'\|_2^2 - \|S_v^{(q)}(x)\|_2^2 - 2\langle h', S_v^{(q)}(x) \rangle \right] \geq (1 + \omega)^{-2}\omega \|h'\|_2^2 \geq 0. \end{aligned}$$

This completes the proof.  $\square$

**Lemma 4.7.** *The condition in the previous lemma holds for  $S_v^{(q)}$ ,  $1 \leq q \leq \infty$  (and even if the  $\ell_q$  norm is replaced by a general norm on  $\mathbb{R}^M$ ).*

*Proof.* First note that by definition (29) and duality we have

$$\|S_v^{(q)}(x)\|_q = (v/2)^{-1} \sup_{k \in B^{q'}(v/2)} \langle k, x - P_{v/2}^{q'} x \rangle$$

A characterization of the orthogonal projection tells us that  $\langle k - P_{v/2}^{q'} x, x - P_{v/2}^{q'} x \rangle \leq 0$  for all  $k \in B^{q'}(v/2)$ , see e.g. [39, Lemma 8]. This gives

$$\begin{aligned} \|S_v^{(q)}(x)\|_q &= (v/2)^{-1} \sup_{k \in B^{q'}(v/2)} \left( \langle k - P_{v/2}^{q'} x, x - P_{v/2}^{q'} x \rangle + \langle P_{v/2}^{q'} x, S_v^{(q)}(x) \rangle \right) \\ &\leq (v/2)^{-1} \langle P_{v/2}^{q'} x, S_v^{(q)}(x) \rangle. \end{aligned}$$

Using once more that  $S_v^{(q)}(x) - x = -P_{v/2}^q(x)$  we further obtain

$$\begin{aligned} &v(\|S_v^{(q)}(x) + h\|_q - \|S_v^{(q)}(x)\|_q) + 2\langle h, S_v^{(q)}(x) - x \rangle \\ &\geq v\|S_v^{(q)}(x) + h\|_q - 2\langle P_{v/2}^{q'} x, S_v^{(q)}(x) \rangle - 2\langle P_{v/2}^{q'} x, h \rangle = v\|S_v^{(q)}(x) + h\|_q - 2\langle P_{v/2}^{q'} x, S_v^{(q)}(x) + h \rangle \\ &\geq v\|S_v^{(q)}(x) + h\|_q - 2\|P_{v/2}^{q'} x\|_{q'} \|S_v^{(q)}(x) + h\|_q \geq 0. \end{aligned}$$

Hereby, we used that  $P_{v/2}^{q'}$  is a projection onto  $B^{q'}(v/2)$ , so  $\|P_{v/2}^{q'} x\|_{q'} \leq v/2$ . This finishes the proof.  $\square$

To summarize we have the following result about weak convergence.

**Corollary 4.8.** Let  $1 \leq q \leq \infty$  and assume that  $(v_\lambda)$  or  $(\omega_\lambda)$  is bounded from below. Then the sequence  $u^{(m)}$  defined in (28) converges weakly to a minimizer of  $K$ , where  $\Psi = \Psi_{v,\omega}^{(q)}$  is the sparsity measure defined in (26). (The  $q$ -norm in (26) can be replaced by any other norm on  $\mathbb{R}^M$ ).

### 4.3 Strong convergence

The next result establishes the strong convergence.

**Proposition 4.9.** *Let  $1 \leq q \leq \infty$  and assume that  $(v_\lambda)$  or  $(\omega_\lambda)$  are bounded away from 0. In case  $(v_\lambda)$  is not bounded away from 0 assume further that there is a constant  $c > 0$  such that  $v_\lambda < c$  for only finitely many  $\lambda$ . Then  $u^{(m)}$  converges strongly to a minimizer of  $K$ .*

*Proof.* The analogues of Lemmas 3.15 and 3.17 in [17] are proven in completely the same way. It remains to justify the analogue of [17, Lemma 3.18]: If for some  $a \in \ell_2(\Lambda, \mathbb{R}^M)$  and some sequence  $(h^{(m)}) \subset \ell_2(\Lambda, \mathbb{R}^M)$  converging weakly to 0 it holds  $\lim_{m \rightarrow \infty} \|U_{v,\omega}^{(q)}(a + h^{(m)}) - U_{v,\omega}^{(q)}(a) - h^{(m)}\|_2 = 0$  then  $\|h^{(m)}\|_2 \rightarrow 0$  for  $m \rightarrow \infty$ . To this end we mainly follow the argument in [17].

Let  $c$  be the constant such that  $v_\lambda < c$  for  $\lambda \in \Lambda_{00}$  for  $\Lambda_{00}$  finite. Then let  $\Lambda_{01}$  be a finite set such that  $\sum_{\lambda \in \Lambda \setminus \Lambda_{01}} \|a_\lambda\|_{q'} \leq \sigma$  for some  $\sigma < c/2$ . (Such a set  $\Lambda_{01}$  exists since  $\|\cdot\|_{q'}$  and

$\|\cdot\|_2$  are equivalent norms on  $\mathbb{R}^M$  and by assumption  $a \in \ell_2(\Lambda, \mathbb{R}^M)$ . Since  $\Lambda_0 = \Lambda_{00} \cup \Lambda_{01}$  is also finite, we have  $\sum_{\lambda \in \Lambda_0} \|h_\lambda^{(m)}\|_2^2 \rightarrow 0$  for  $m \rightarrow \infty$  by the weak convergence of  $h^{(m)}$  to 0. Thus, we are left with proving that  $\sum_{\lambda \in \Lambda \setminus \Lambda_0} \|h_\lambda^{(m)}\|_2^2 \rightarrow 0$  for  $m \rightarrow \infty$ .

For each  $m$  we split  $\Lambda_1 := \Lambda \setminus \Lambda_0$  into the subsets  $\Lambda_{1,m} := \{\lambda \in \Lambda_1 : \|h_\lambda^{(m)} + a_\lambda\|_{q'} < v_\lambda/2\}$  and  $\tilde{\Lambda}_{1,m} = \Lambda_1 \setminus \Lambda_{1,m}$ . If  $\lambda \in \Lambda_1$  then  $U_{v,\omega}^{(q)}(a + h^{(m)})_\lambda = U_{v,\omega}^{(q)}(a)_\lambda = 0$  since  $\|a_\lambda + h_\lambda^{(m)}\|_{q'}, \|a_\lambda\|_{q'} \leq v_\lambda/2$ . Thus,  $\|h_\lambda^{(m)} - U_{v,\omega}^{(q)}(a + h^{(m)})_\lambda + U_{v,\omega}^{(q)}(a)_\lambda\|_2^2 = \|h_\lambda^{(m)}\|_2^2$  and by assumption,

$$\sum_{\lambda \in \Lambda_1} \|h_\lambda^{(m)}\|_2^2 \leq \|h^{(m)} - U_{v,\omega}^{(q)}(a + h^{(m)}) + U_{v,\omega}^{(q)}(a)\|_2^2 \rightarrow 0 \quad \text{as } m \rightarrow \infty.$$

Now let  $\lambda \in \tilde{\Lambda}_{1,m}$ . We first consider the case that  $\omega_\lambda = 0$ , i.e.,  $U_{v,\omega} q(x)_\lambda = S_v^{(q)}(x)_\lambda$ . Since  $\|a_\lambda\|_{q'} \leq \sigma < v_\lambda/2$  we have  $S_v^{(q)}(a) = 0$ , and thus,

$$\begin{aligned} \|h_\lambda^{(m)} - S_{v_\lambda}^{(q)}(h_\lambda^{(m)} + a_\lambda)\|_{q'} &= \|h_\lambda^{(m)} - (h_\lambda^{(m)} + a_\lambda) + P_{v_\lambda/2}^{q'}(h_\lambda^{(m)} + a_\lambda)\|_{q'} \\ &= \|P_{v_\lambda/2}^{q'}(h_\lambda^{(m)} + a_\lambda) - a_\lambda\|_{q'} \geq \|P_{v_\lambda/2}^{q'}(h_\lambda^{(m)} + a_\lambda)\|_{q'} - \|a_\lambda\|_{q'} \geq v_\lambda/2 - \sigma \geq c/2 - \sigma. \end{aligned}$$

Hereby, we used that  $\|P_{v_\lambda/2}^{q'}(h_\lambda^{(m)} + a_\lambda)\|_{q'} = v_\lambda/2$  (because  $\|h_\lambda^{(m)} + a_\lambda\|_{q'} \geq v_\lambda/2$ ). Since every norm on a finite-dimensional space is equivalent there is a constant  $C$  such that

$$\|h_\lambda^{(m)} - S_{v_\lambda}^{(q)}(h_\lambda^{(m)} + a_\lambda) + S_{v_\lambda}^{(q)}(a_\lambda)\|_2^2 \geq C^2(c/2 - \sigma)^2 > 0.$$

However, since by assumption  $\sum_{\lambda \in \Lambda} \|h_\lambda^{(m)} - S_{v_\lambda}^{(q)}(h_\lambda^{(m)} + a_\lambda) + S_{v_\lambda}^{(q)}(a)\|_2^2 \rightarrow 0$  as  $m \rightarrow \infty$  there must exist an  $m_0$  such that  $\tilde{\Lambda}_{1,m}$  is empty for all  $m \geq m_0$ .

In the case that  $\omega_\lambda$  does not vanish we have

$$\begin{aligned} \|h_\lambda^{(m)} - U_{v,\omega}^{(q)}(h_\lambda^{(m)} + a)_\lambda + U_{v,\omega}^{(q)}(a)_\lambda\|_2 &= \|h_\lambda^{(m)} - (1 + \omega_\lambda)^{-1} S_{v_\lambda}^{(q)}(h_\lambda^{(m)} + a_\lambda)\|_2 \\ &= (1 + \omega_\lambda)^{-1} \|(1 + \omega_\lambda) h_\lambda^{(m)} - S_{v_\lambda}^{(q)}(h_\lambda^{(m)} + a_\lambda)\|_2 \end{aligned} \quad (34)$$

We claim that

$$\|(1 + \omega_\lambda) h_\lambda^{(m)} - S_{v_\lambda}^{(q)}(h_\lambda^{(m)} + a_\lambda)\|_2 \geq \|h_\lambda^{(m)} - S_{v_\lambda}^{(q)}(h_\lambda^{(m)} + a_\lambda)\|_2 \quad (35)$$

so that we can apply the argument for  $\omega_\lambda = 0$  to conclude that  $\tilde{\Lambda}_{1,m}$  is empty for  $m$  sufficiently large. Let us omit for the moment all indexes  $\lambda$  and  $m$  for the sake of simpler notation. We have

$$\|(1 + \omega)h - S_v^{(q)}(h + a)\|_2^2 - \|h - S_v^{(q)}(h + a)\|_2^2 = 2\omega \langle h, h - S_v^{(q)}(h + a) \rangle + \omega^2 \|h\|_2^2 \quad (36)$$

and furthermore,

$$\begin{aligned} \langle h, h - S_v^{(q)}(h + a) \rangle &= \langle h, P_{v/2}^{q'}(h + a) - a \rangle \\ &= -\langle h + a - P_{v/2}^{q'}(h + a), a - P_{v/2}^{q'}(h + a) \rangle + \|a - P_{v/2}^{q'}(h + a)\|_2^2 \geq 0. \end{aligned} \quad (37)$$



Hereby, we used that  $a \in B^{q'}(\sigma) \subset B^{q'}(v/2)$  and the fact that  $\langle k - P_{v/2}^{q'}(x), x - P_{v/2}^{q'}(x) \rangle \leq 0$  for all  $k \in B^{q'}(v/2)$  and  $x \in \mathbb{R}^M$ . Thus, the term in (36) is non-negative and therefore our claim (35) holds.  $\square$

Let us shortly comment on the condition that if  $v_\lambda$  is not bounded from below there is at least some  $c > 0$  such that  $v_\lambda > c$  except for a finite set of indexes  $\lambda$ . This condition is mainly relevant when considering also a minimization over  $(v_\lambda)$ . Then the term  $\sum \theta_\lambda (\rho_\lambda - v_\lambda)^2$  in the functional  $J(u, v)$  ensures that the sequence  $(\rho_\lambda - v_\lambda)$  is contained in  $\ell_{2, \theta^{1/2}}$ . If  $\theta_\lambda$  and  $\rho_\lambda$  are bounded from below this implies that  $v_\lambda$  can be less than  $1/2 \min_\lambda \rho_\lambda$ , say, only for finitely many  $\lambda$ .

## 5 Numerical Implementation and Error Analysis

The scope of this section is twofold: We want to formulate an implementable version of the double-minimization algorithm and show its strong convergence. To this end we develop an error analysis.

### 5.1 Numerical implementation

Let us compose the two iterative algorithms described in (11) and (28), respectively, into a unique scheme.

#### Algorithm 1. JOINTSPARSE

*Input:* Data vector  $(g_j)_{j=1}^N$ , initial points  $u^{(0)} \in \ell_2(\Lambda, \mathbb{R}^M)$ ,  $v^{(0)}$  with  $0 \leq v_\lambda^{(0)} \leq \rho_\lambda$ , number  $n_{\max}$  of outer iterations, number of inner iterations  $L_n$ ,  $n = 1, \dots, n_{\max}$ .

*Parameters:*  $q \in [1, \infty]$ , positive weights  $(\theta_\lambda)$ ,  $(\rho_\lambda)$ ,  $(\omega_\lambda)$  with  $\omega_\lambda \geq c > 0$ , such that  $\Phi^{(q)}$  and hence  $J$  are convex, see Proposition 2.1

*Output:* Approximation  $(u^*, v^*)$  of the minimizer of  $J_{\theta, \rho, \omega}^{(q)}$

```

 $u^{(0,0)} := u^{(0)}$ ;
for  $n := 0$  to  $n_{\max}$  do
  for  $m := 0$  to  $L_n$  do
     $u^{(n,m+1)} := U_{v^{(n)}, \omega}^{(q)}(u^{(n,m)} + T^*(g - Tu^{(n,m)}))$ ;
  endfor
   $u^{(n+1,0)} := u^{(n, L_n)}$ ;
   $v^{(n+1)} := \left( \begin{array}{l} \rho_\lambda - \frac{1}{2\theta_\lambda} \|u^{(n+1,0)}\|_q, \quad \|u^{(n+1,0)}\|_q < 2\theta_\lambda \rho_\lambda \\ 0, \quad \text{otherwise} \end{array} \right)_{\lambda \in \Lambda}$ ;
endfor
 $u^* := u^{(n_{\max}, L_{n_{\max}})}$ ;
 $v^* := v^{(n_{\max})}$ .

```

Observe that each (inner) iteration of the above algorithm involves an application of  $T^*T$  and of the thresholding operator  $U_{v, \omega}^{(q)}$ . The latter can be applied fast. So if there is also a fast algorithm for the computation of  $T^*T$  then each iteration can be done fast.

Our analysis ensures the (weak) convergence of this scheme only if the inner loop computes exactly the minimizer of  $J(u, v^{(n)})$  for fixed  $v^{(n)}$ , i.e., if  $L_n = \infty$ . Of course, this cannot be numerically realized, so we need to analyze what happens if the inner loop makes a small error in computing this minimizer. In other words, how large do we have to choose  $n_{\max}$  and  $L_n, n = 1, \dots, n_{\max}$  in order to ensure that we have approximately computed the minimizer  $u^*, v^*$  within a given error tolerance?

## 5.2 Error analysis and strong convergence of JOINTSPARSE

First of all we want to establish the convergence rate of the inner loop, i.e., the iterative thresholding algorithm of the previous Section.

**Proposition 5.1.** *Assume that  $\omega_\lambda \geq \gamma > 0$  for all  $\lambda \in \Lambda$  (implying that  $K(u) = K_{v,\omega}^{(q)}(u)$  is strictly convex) and  $\|T\| < 1$ . Set  $\alpha := (1 + \gamma)^{-1} \|I - T^*T\| < 1$ . Then the iterative thresholding algorithm*

$$u^{(n,m+1)} := U_{v^{(n)},\omega}^{(q)} \left( u^{(n,m)} + T^*(g - Tu^{(n,m)}) \right),$$

converges linearly

$$\|u^{(n,\infty)} - u^{(n,m+1)}\|_2 \leq \alpha \|u^{(n,\infty)} - u^{(n,m)}\|_2. \quad (38)$$

*Proof.* Note that

$$u^{(n,\infty)} := U_{v^{(n)},\omega}^{(q)} \left( u^{(n,\infty)} + T^*(g - Tu^{(n,\infty)}) \right).$$

By non-expansiveness of  $S_v^{(q)}$  (see Lemma 4.4 and its proof) we obtain

$$\begin{aligned} & \|u^{(n,\infty)} - u^{(n,m+1)}\|_2 \\ &= \|U_{v^{(n)},\omega}^{(q)} \left( u^{(n,\infty)} + T^*(g - Tu^{(n,\infty)}) \right) - U_{v^{(n)},\omega}^{(q)} \left( u^{(n,m)} + T^*(g - Tu^{(n,m)}) \right)\|_2 \\ &= \left( \sum_{\lambda \in \Lambda} (1 + \omega_\lambda)^{-2} \|S_{v_\lambda}^{(q)}((u^{(n,\infty)} + T^*(g - Tu^{(n,\infty)}))_\lambda) - S_{v_\lambda}^{(q)}((u^{(n,m)} + T^*(g - Tu^{(n,m)}))_\lambda)\|_2^2 \right)^{1/2} \\ &\leq \sup_{\lambda \in \Lambda} (1 + \omega_\lambda)^{-1} \|(I - T^*T)(u^{(n,\infty)} - u^{(n,m)})\|_2 \leq (1 + \gamma)^{-1} \|I - T^*T\| \|u^{(n,\infty)} - u^{(n,m)}\|_2 \\ &= \alpha \|u^{(n,\infty)} - u^{(n,m)}\|_2. \end{aligned}$$

This establishes the claim.  $\square$

*Remark:* Clearly, the error estimation in (38) holds also if one is only interested in analyzing the iterative thresholding algorithm from the last section (i.e. without doing the outer iteration). Then it might also be interesting to consider the case that  $\omega = 0$ . According to what we have proven in the previous section the algorithm still converges provided the weight  $v$  is bounded away from zero. However, then the error estimation (5.1) has a useful meaning only if  $\alpha = \|I - T^*T\| < 1$ . So this applies if  $T^*T$  is boundedly invertible. For a usual inverse problem, however, we will have a non-invertible  $T$  or at least one with unbounded inverse resulting in  $\|I - T^*T\| = 1$ . So in this case we only know that the algorithm converges, but an error estimate does not seem to be available.

For simplicity we restrict the following error analysis to the most interesting cases  $q \in \{1, 2, \infty\}$ . We first need the following technical result.

**Lemma 5.2.** For  $q \in \{1, 2, \infty\}$  the projection  $P_v^q$  onto the ball  $B^q(v) \subset \mathbb{R}^M$  is a Lipschitz function with respect to  $v \in \mathbb{R}_+$ . In particular, we have

$$\|P_v^q(x) - P_w^q(x)\|_{\ell_2^M} \leq L|v - w| \quad \text{for all } x \in \mathbb{R}^M, \quad (39)$$

where  $L = 1$  for  $q = 2$  and  $L = M^{1/2}$  for  $q \in \{1, \infty\}$ .

*Proof.* Let us start with  $q = 2$ . By distinguishing cases it is not difficult to show that

$$\|P_v^2(x) - P_w^2(x)\|_{\ell_2^M} \leq |v - w|.$$

For  $q = \infty$  we have  $P_v^\infty(x) = (p_v^\infty(x_\ell))_{\ell=1}^M$  where for  $y \in \mathbb{R}$

$$p_v^\infty(y) = \begin{cases} y & \text{if } |y| \leq v, \\ y - \text{sign}(y)(|y| - v) & \text{otherwise.} \end{cases}$$

Since  $p_v^\infty$  can be interpreted as a projection onto the  $\ell_2$  ball in dimension 1, we obtain that

$$|p_v^\infty(y) - p_w^\infty(y)| \leq |v - w|,$$

and

$$\|P_v^\infty(x) - P_w^\infty(x)\|_{\ell_2^M} = \left( \sum_{\ell=1}^M |p_v^\infty(x_\ell) - p_w^\infty(x_\ell)|^2 \right)^{1/2} \leq M^{1/2}|v - w|.$$

The case  $q = 1$  requires a bit more effort. By Lemma 4.2 (c) we have the following. Let  $x_{i_k}$  denote the reordering of the entries of  $x$  by magnitude as in Lemma 4.2. Let  $n \in \{1, \dots, M\}$  be the largest index satisfying

$$|x_{i_n}| \geq \frac{1}{n-1} \left( \sum_{k=1}^{n-1} |x_{i_k}| - v \right).$$

Then

$$\begin{aligned} (P_v^1(x))_{i_j} &= x_{i_j} - \frac{\text{sign}(x_{i_j})}{n} \left( \sum_{k=1}^n |x_{i_k}| - v \right), \quad j = 1, \dots, n, \\ (P_v^1(x))_{i_j} &= 0, \quad j = n+1, \dots, M. \end{aligned}$$

Observe first that for all  $x \in \mathbb{R}^M$  there exists  $\varepsilon_0 > 0$  such that for all  $0 < \varepsilon < \varepsilon_0$  the same  $n \in \{1, \dots, M\}$  is the largest index satisfying

$$|x_{i_n}| \geq \frac{1}{n-1} \left( \sum_{k=1}^{n-1} |x_{i_k}| - (v + \varepsilon) \right).$$

For  $0 < \varepsilon < \varepsilon_0$ , a simple computation yields

$$\frac{(P_{v+\varepsilon}(x) - P_v(x))_{i_j}}{\varepsilon} = \begin{cases} \frac{\text{sign}(x_{i_j})}{n} & \text{for } j = 1, \dots, n, \\ 0 & j = n+1, \dots, M. \end{cases}$$

This means that the map  $v \rightarrow P_v^1(x)$  is right-differentiable, i.e., the limit

$$(P_v^1(x))'_+ = \lim_{\varepsilon \rightarrow 0_+} \frac{P_{v+\varepsilon}^1(x) - P_v^1(x)}{\varepsilon}$$

exists in  $\mathbb{R}^M$ . Moreover, it also follows that

$$\|(P_v^1(x))'_+\|_2 = \sqrt{n} \leq \sqrt{M}. \quad (40)$$

To conclude the proof we use the following standard result.

**Lemma 5.3.** *Let  $f : \mathbb{R} \rightarrow \mathbb{R}^M$  and  $\varphi : \mathbb{R} \rightarrow \mathbb{R}$  be two continuous and right differentiable functions such that*

$$\|f'_+(v)\| \leq \varphi'_+(v),$$

for all  $v \in \mathbb{R}$ . Then

$$\|f(v) - f(w)\| \leq \varphi(v) - \varphi(w), \quad \text{for all } v \geq w.$$

According to the notation of this latter lemma, let us set  $f(v) = P_v^1(x)$  and  $\varphi(v) = M^{1/2}v$ . Since  $P_v^1(x)$  is a continuous function with respect to  $v$  (in fact this is true for any projection onto convex sets, see [37]), by (40) and an application of the lemma we conclude that  $\|P_v^1(x) - P_w^1(x)\| \leq M^{1/2}|v - w|$ .  $\square$

Observe that the strict convexity of  $\Phi^{(q)}(u, v)$  is equivalent to  $\theta_\lambda \omega_\lambda > \kappa/4$ , see Proposition 2.1. In the following Proposition we require the slightly stronger condition that  $\theta_\lambda \omega_\lambda$  is bounded strictly away from  $\kappa/4$ , at least for  $q = 1, 2$ .

**Proposition 5.4.** *Let  $q \in \{1, 2, \infty\}$ . Assume that  $\theta_\lambda \omega_\lambda \geq \sigma > \phi_q/4$  for all  $\lambda \in \Lambda$ , where  $\phi_1 = M$ ,  $\phi_2 = 1$ ,  $\phi_\infty = \sqrt{M}$ , implying that  $\Phi^{(q)}(u, v)$  and  $J(u, v)$  are strictly convex, see Proposition 2.1. Moreover, let us assume that  $\omega_\lambda \geq \gamma > 0$  for all  $\lambda \in \Lambda$ . Suppose  $\|T\| < 1$  resulting in  $\|I - T^*T\| \leq 1$ . Set*

$$\beta := \sup_{\lambda \in \Lambda} \frac{\phi_q}{4\theta_\lambda \omega_\lambda + 4\theta_\lambda(1 - \|I - T^*T\|)} \leq \frac{\phi_q}{4\sigma} < 1. \quad (41)$$

Then for each  $n \in \mathbb{N}$  one has the following error estimate

$$\|u^{(n, \infty)} - u^*\|_{\ell_2(\Lambda, \mathbb{R}^M)} \leq \beta \|u^{(n, 0)} - u^*\|_{\ell_2(\Lambda, \mathbb{R}^M)}.$$

*Proof.* Let us consider the  $n$ -th iteration of the outer loop. We have

$$u^{(n, \infty)} = U_{v^{(n)}, \omega}^{(q)} \underbrace{(u^{(n, \infty)} + T^*(g - Tu^{(n, \infty)}))}_{:=y^{(n)}}.$$

By the weak convergence of the double-minimization algorithm, also the minimum solution  $u^*$  satisfies a similar relation,

$$u^* = U_{v^*, \omega}^{(q)} \underbrace{(u^* + T^*(g - Tu^*))}_{:=y^*}.$$

Recall that  $U_{v,\omega}^{(q)}(y)_\lambda := (1 + \omega_\lambda)^{-1} S_{v_\lambda}^{(q)}(y_\lambda)$ . By non-expansiveness of  $S_v^{(q)}$  (Lemma 4.4) we have

$$\begin{aligned} \|u_\lambda^{(n,\infty)} - u_\lambda^*\|_2 &\leq \|U_{v^{(n)},\omega}^{(q)}(y^{(n)})_\lambda - U_{v^{(n)},\omega}^{(q)}(y^*)_\lambda\|_2 + \|U_{v^{(n)},\omega}^{(q)}(y^*)_\lambda - U_{v^*,\omega}^{(q)}(y^*)_\lambda\|_2 \\ &= (1 + \omega_\lambda)^{-1} \|y_\lambda^{(n)} - y_\lambda^*\|_2 + \|U_{v^{(n)},\omega}^{(q)}(y^*)_\lambda - U_{v^*,\omega}^{(q)}(y^*)_\lambda\|_2 \\ &\leq (1 + \omega_\lambda)^{-1} \|I - T^*T\| \|u_\lambda^{(n,\infty)} - u_\lambda^*\|_2 + \|U_{v^{(n)},\omega}^{(q)}(y^*)_\lambda - U_{v^*,\omega}^{(q)}(y^*)_\lambda\|_2. \end{aligned}$$

This implies

$$\begin{aligned} \|u_\lambda^{(n,\infty)} - u_\lambda^*\|_2 &\leq (1 - (1 + \omega_\lambda)^{-1} \|I - T^*T\|)^{-1} \|U_{v^{(n)},\omega}^{(q)}(y^*)_\lambda - U_{v^*,\omega}^{(q)}(y^*)_\lambda\|_2 \\ &= (1 + \omega_\lambda - \|I - T^*T\|)^{-1} \|S_{v_\lambda^{(n)}}(y_\lambda^*) - S_{v_\lambda^*}(y_\lambda^*)\|_2. \end{aligned}$$

Recall from Lemma 4.1 that  $S_v^{(q)}(2)(x) = x - P_{v/2}^q(x)$  where  $P_{v/2}^q$  denotes the orthogonal projection of  $x$  onto the  $\ell_q$ -ball of radius  $v/2$ . By Lemma 5.2 we have that for any  $z \in \mathbb{R}^M$

$$\|S_{v_\lambda^{(n)}}^{(q)}(z) - S_{v_\lambda^*}^{(q)}(z)\|_2 = \|P_{v_\lambda^{(n)}/2}^q(z) - P_{v_\lambda^*/2}^q(z)\|_2 \leq \frac{L}{2} |v_\lambda^{(n)} - v_\lambda^*|.$$

So  $S_v^{(q)}(z)$  is also Lipschitz in  $v$ . Let us recall that

$$v_\lambda^{(n)} := \begin{cases} \rho_\lambda - \frac{1}{2\theta_\lambda} \|u_\lambda^{(n,0)}\|_q, & \|u_\lambda^{(n,0)}\|_q < 2\theta_\lambda \rho_\lambda \\ 0, & \text{otherwise.} \end{cases}$$

and

$$v_\lambda^* := \begin{cases} \rho_\lambda - \frac{1}{2\theta_\lambda} \|u_\lambda^*\|_q, & \|u_\lambda^*\|_q < 2\theta_\lambda \rho_\lambda \\ 0, & \text{otherwise.} \end{cases}$$

By distinguishing cases we can show that

$$|v_\lambda^{(n)} - v_\lambda^*| \leq \frac{1}{2\theta_\lambda} \left| \|u_\lambda^{(n,0)}\|_q - \|u_\lambda^*\|_q \right| \leq \frac{1}{2\theta_\lambda} \|u_\lambda^{(n,0)} - u_\lambda^*\|_q \leq \frac{R}{2\theta_\lambda} \|u_\lambda^{(n,0)} - u_\lambda^*\|_2,$$

where  $R = 1$  for  $q \in \{2, \infty\}$  and  $R = M^{-1/2}$  for  $q = 1$ . Pasting the pieces together yields

$$\|u_\lambda^{(n,\infty)} - u_\lambda^*\|_2 \leq \frac{\phi_q}{4\theta_\lambda (\omega_\lambda + 1 - \|I - T^*T\|)} \|u_\lambda^{(n,0)} - u_\lambda^*\|_2 \leq \beta \|u_\lambda^{(n,0)} - u_\lambda^*\|_2.$$

Summation over  $\lambda \in \Lambda$  completes the proof.  $\square$

Let us combine the previous two results to obtain the error estimation for the finite algorithm, i.e., for  $L_n < \infty$ .

**Theorem 5.5.** *Make the same assumptions as in Propositions 5.1 and 5.4. Choose  $L_n$  such that*

$$\delta_n := (\alpha^{L_n} (1 + \beta) + \beta) \leq \delta < 1 \quad \text{for all } n \in \mathbb{N}.$$

*(This is possible since  $\alpha, \beta < 1$ ). Then we have linear convergence of our algorithm, i.e.,*

$$\|u^{(n,0)} - u^*\|_2 \leq \delta_n \|u^{(n-1,0)} - u^*\|_2.$$

*Proof.* Using Proposition 5.1 and Proposition 5.4 we get

$$\begin{aligned}
\|u^{(n,0)} - u^*\|_2 &\leq \|u^{(n,0)} - u^{(n-1,\infty)}\|_2 + \|u^{(n-1,\infty)} - u^*\|_2 \\
&\leq \alpha^{L_{n-1}} \|u^{(n-1,0)} - u^{(n-1,\infty)}\|_2 + \beta \|u^{(n-1,0)} - u^*\|_2 \\
&\leq \alpha^{L_{n-1}} \left( \|u^{(n-1,0)} - u^*\|_2 + \|u^* - u^{(n-1,\infty)}\|_2 \right) + \beta \|u^{(n-1,0)} - u^*\|_2 \\
&\leq \alpha^{L_{n-1}} \left( \|u^{(n-1,0)} - u^*\|_2 + \beta \|u^{(n-1,0)} - u^*\|_2 \right) + \beta \|u^{(n-1,0)} - u^*\|_2 \\
&\leq (\alpha^{L_{n-1}}(1 + \beta) + \beta) \|u^{(n-1,0)} - u^*\|_2.
\end{aligned}$$

This concludes the proof.  $\square$

*Remark:* The last theorem shows that it is possible to choose the number  $L_n$  of inner iterations constant with respect to  $n$ .

### 5.3 Strong convergence of the double-minimization algorithm

Finally, we can establish the strong convergence of the double-minimization algorithm and conclude the full proof of Theorem 3.1.

**Corollary 5.6.** Under the assumptions of Proposition 5.4, if the minimizer of  $J(u, v^{(n)})$  for fixed  $v^{(n)}$  could be computed exactly, i.e.,  $L_n = \infty$  for all  $n \in \mathbb{N}$ , then the outer loop converges with exponential rate, and we have

$$\|u^{(n)} - u^*\|_2 \leq \beta^n \|u^{(0)} - u^*\|_2,$$

where we have denoted here  $u^{(n)} := u^{(n,\infty)}$ . Moreover, the sequence  $v^{(n)}$  converges componentwise and  $v^{(n)} - v^*$  converges to 0 strongly in  $\ell_{2,\theta}(\Lambda)$ .

*Proof.* The first part of the statement is a direct application of Proposition 5.4. It remains to show that  $v^{(n)} - v^*$  converges to 0 strongly in  $\ell_{2,\theta}(\Lambda)$ . Using that all norms on  $\mathbb{R}^M$  are equivalent it follows that

$$\begin{aligned}
4 \sum_{\lambda \in \Lambda} \theta_\lambda^2 |v^{(n)} - v^*|^2 &= \sum_{\lambda \in \Lambda} \left| \|u_\lambda^*\|_q - \|u_\lambda^{(n)}\|_q \right|^2 \leq \sum_{\lambda \in \Lambda} \|u_\lambda^* - u_\lambda^{(n)}\|_q^2 \\
&\leq C \sum_{\lambda \in \Lambda} \|u_\lambda^* - u_\lambda^{(n)}\|_2^2 = C \|u^* - u^{(n)}\|_{\ell_2(\Lambda, \mathbb{R}^M)}^2.
\end{aligned}$$

Thus,  $v^{(n)} - v^{(\infty)}$  converges also strongly in  $\ell_{2,\theta}(\Lambda)$ .  $\square$

## 6 Color image reconstruction

With this section we illustrate the application of the algorithms for color image recovery. The scope is to furnish a qualitative description of the behavior of the scheme. In a subsequent work we plan to provide a finer quantitative analysis in the context of *distributed compressed sensing* [3].

We begin by illustrating an interesting real-world problem occurring in art restoration. On 11<sup>th</sup> March 1944, a group of bombs launched from an Allied airplane hit the famous

Italian Eremitani’s Church in Padua, destroying it together with the inestimable frescoes by Andrea Mantegna *et al.* contained in the Ovetari Chapel. Details on “the state of the art” can be found in [28, 27]. In 1920 a collection of high quality gray level pictures of these frescoes has been made by Alinari. The only color images of the frescoes are dated to 1940, but unfortunately their quality (i.e., the intrinsic resolution of the printouts) is much lower, see Figure 6. Inspired by the fresco application, we model the problem of the recovery of a high resolution color image from a low resolution color datum and a high resolution gray datum. We will implement the solution to the model problem as a non-trivial application of the algorithms we have presented in this paper.

## 6.1 Color images, curvelets, and joint sparsity

Let us assume that the color images are encoded into YIQ channels. The Y component represents the luminance information (gray level), while I and Q give the chrominance information. Of course, one may also choose a different encoding system, e.g., RGB or CMYK. Clearly, the color image  $f = (f_1, f_2, f_3)$  can be represented as a 3-channel signal. In order to apply our algorithm, we need to fix a frame for which we can assume color images being jointly sparse.

It is well-known that *curvelets* [9] are well-suited for sparse approximations of curved singularities. A natural image can in fact be modelled as a function which is piecewise smooth except on a discontinuity set, the latter being described as the union of rectifiable curves. Moreover, there are fast algorithms available for the computation of curvelet coefficients of digital images [8].

In the following, let us assume that a color image  $f$  is encoded into a vector of curvelet coefficients  $(u_\lambda^\ell)_{\lambda \in \Lambda}^{\ell=1,2,3}$ . The image can be reconstructed by the synthesis formula

$$f = (Fu^\ell)_{\ell=1,2,3} := \left( \sum_{\lambda \in \Lambda} u_\lambda^\ell \psi_\lambda \right)_{\ell=1,2,3},$$

where  $\{\psi_\lambda : \lambda \in \Lambda\}$  is the collection of curvelets. The index  $\lambda$  consists of 3 different parameters,  $\lambda = (j, p, k)$ , where  $j$  corresponds to scale,  $p$  to a rotation, and  $k$  to the spatial location of the curvelet  $\psi_\lambda$ . We do not enter in further details, especially of the discrete and numerical implementation, which one can find in [9, 8].

Let us instead observe that significant curvelet coefficients  $u_\lambda = (u_\lambda^1, u_\lambda^2, u_\lambda^3)$  will appear simultaneously at the same  $\lambda \in \Lambda$  for all the channels, as soon as the corresponding curvelet overlaps with a (curved) singularity (appearing simultaneously in all the channels), and is approximately tangent to it. This justifies the joint sparsity assumption for color images with respect to curvelets.

## 6.2 The model of the problem

The datum of our problem is a three-channel signal  $g = (g_1, g_2, g_3) \in \ell_2(\mathbb{Z}_{N_0}^2, \mathbb{R}^3)$  where  $g_i$ ,  $i = 2, 3$ , are the low resolution chrominance channels I and Q, and  $g_1$  is the high resolution gray channel Y. We assume that  $g$  was produced by  $g = Tu$  where  $u = (u^1, u^2, u^3)$  are the curvelet coefficients of the three channels of the high resolution color image that we want



Figure 1: *Left:* The low-resolution color image is here presented after Gaussian filtering and downsampling. In the numerical experiments the I and Q channels are used. *Right:* The high resolution gray level image encodes several morphological information useful to recover the high resolution color image.

to reconstruct. The operator  $T = (T_{\ell,j})_{\ell,j=1,2,3}$  can be expressed by the matrix

$$T = \begin{pmatrix} F & 0 & 0 \\ 0 & AF & 0 \\ 0 & 0 & AF \end{pmatrix}. \quad (42)$$

Here,  $A$  is the linear operator that transforms the high-resolution image into the low resolution image. In particular,  $A$  can be taken as a convolution operator (with a Gaussian for instance) followed by downsampling. Eventually, we may assume a suitable scaling in order to make  $\|T\| < 1$ , and a different weighting of the gray channel and the I,Q channel in the discrepancy term. Since  $A$  is not invertible, also the operator  $T$  is not invertible, and the minimization of  $\mathcal{T}(u)$  requires a regularization. Clearly, for this task we use the functional  $K$  defined in (4) or  $J$  defined in (5).

### 6.3 On the choice of the parameters

What remains to clarify is the choice of the parameters  $\omega_\lambda$ ,  $\theta_\lambda$ , and  $\rho_\lambda$ . The parameter  $\omega_\lambda \geq \gamma > 0$  has been introduced for the sole purpose to make  $J$  strictly convex. A large value of this parameter actually produces an image  $u$  which is significantly blurred and no information about edges is recovered. Thus, we rather put  $\omega_\lambda = \gamma = \varepsilon > 0$  small. Due to the convexity requirements (see Subsection 2.3), we select  $\theta_\lambda \sim \frac{M}{\varepsilon}$ . The choice of  $\rho_\lambda$  requires a deeper understanding of the information encoded by the curvelet coefficients.

Indeed, in [9] it was observed that those curvelets that overlap with a discontinuity decay like  $\|u_\lambda\|_q \lesssim 2^{-3/4j}$  while the others satisfy  $\|u_\lambda\|_q \lesssim 2^{-3/2j}$  (where  $j$  denotes the scale). Since we want to recover joint discontinuities we may choose  $\rho_\lambda := \rho_{j,p,k} \sim 2^{-js}$  with  $s \in [3/4, 3/2]$ . By this choice and by (12) the locations  $\lambda$  for which  $v_\lambda = 0$  will indicate a potential joint discontinuity.

Of course, this is just one possible choice of the parameters and further information might be extracted from the joint sparsity pattern indicated by  $v$ , by the use of different parameters. We believe that a deeper study of the characterization of the morphological



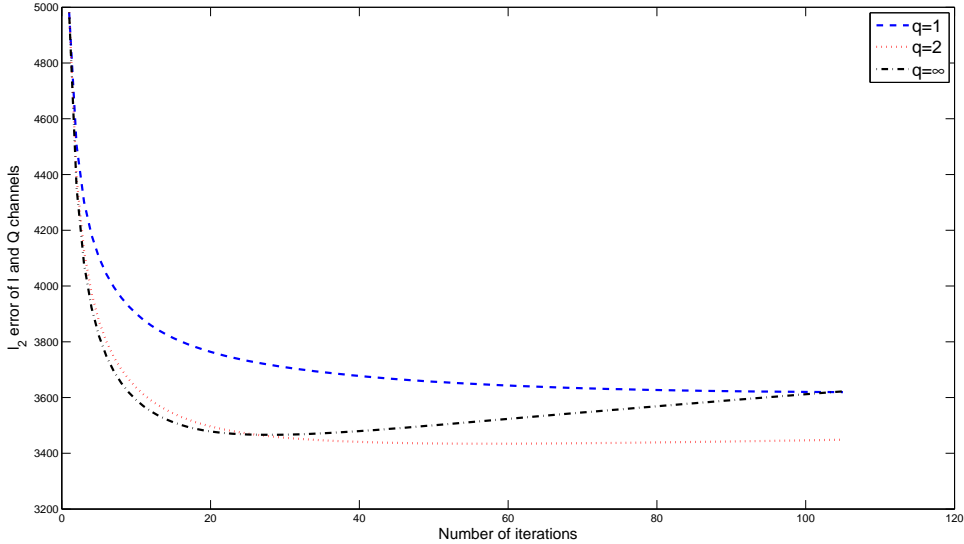


Figure 2: The  $\ell_2$  error between the *original color image* and the iterations of the algorithm is shown for different values of  $q = 1, 2, \infty$ . We have considered  $L_n = 105$  and  $n_{\max} = 1$ , the numbers of inner and outer iterations respectively. We have fixed here  $\omega_\lambda = 0$ ,  $\theta_\lambda = 10$ , and  $\rho_\lambda = 20 \times 2^{-j}$ .

properties of signals encoded by frames (e.g., curvelets and wavelets) is fundamental for the right choice of these parameters. We refer to [30, 31] for deeper insights in this direction, concerning fine properties of functions encoded by the distribution of wavelet coefficients.

## 6.4 Numerical experiments

According to the previous subsections, we illustrate here the application of **JOINTSPARSE** for the recovery of a high resolution color image from a low resolution color datum and a high resolution gray datum. In Figure 1 we illustrate the data of the problem. In this case the resolution of the color image has been reduced by a factor of 4 in each direction by using a Gaussian filter and a downsampling. We have conducted several experiments for different choices of  $q \in \{1, 2, \infty\}$ , with fixed parameters as indicated in Subsection 6.3. We have chosen  $L_n = 105$  and  $n_{\max} = 1$ , as well as  $L_n = 7$  and  $n_{\max} = 15$  (the numbers of inner and outer iterations, respectively). In the first case, only the minimization of  $J(u, v^{(0)})$  with respect to  $u$  has been performed, i.e., no iterative adaptation of the joint sparsity pattern indicated by  $v$  occurred. In order to estimate the different behavior depending of the parameters above, we have evaluated at each iteration the  $\ell_2$ -error between the reconstructed I and Q color channels and the *original* I and Q color channels. Figures 2 and 3 indicate that the error decreases for increasing values of  $q$ . This means that the increased coupling due to the  $q$ -parameter is significant in order to improve the recovery. Recall that the choice  $q = 1$  does not induce any coupling between channels.

This coupling effect due to  $q > 1$  is even more evident in Figure 3, where the adaptation

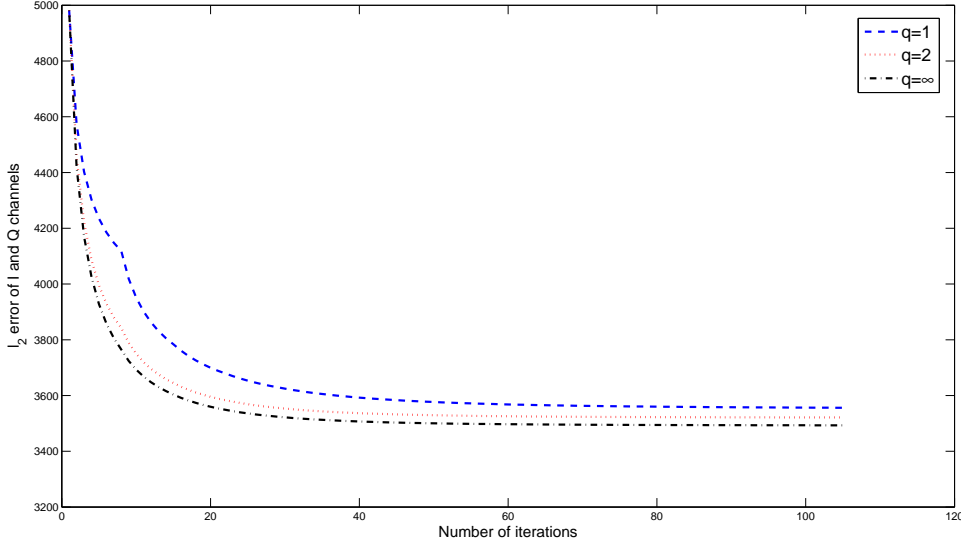


Figure 3: The  $\ell_2$  error between the *original color image* and the iterations of the algorithm is shown for different values of  $q = 1, 2, \infty$ . We have considered  $L_n = 7$  and  $n_{\max} = 15$ , the numbers of inner and outer iterations respectively. We have fixed here  $\omega_\lambda = 1/20$ ,  $\theta_\lambda = 10$ , and  $\rho_\lambda = 20 \times 2^{-j}$ .

of the weight  $v$  occurs. The left and the central pictures in the second row of Figure 5 show a reduced color distortion at edges, passing from the case  $q = 1$  (without coupling) to the case  $q = \infty$  respectively, and consequently a better edge resolution. Nevertheless, the differences are not so remarkable. This is due to the fact that, although the functional  $J$  promotes coupling at edges, it does not necessarily enforce a significant edge enhancement. Thus, we may modify the functional by adding an additional total variation constraint on the I and Q channels:

$$J_{\text{TV}}(u, v) := J(u, v) + (|Fu^2|_{\text{TV}} + |Fu^3|_{\text{TV}}).$$

The effect of this modification is to promote edge enhancing together with their simultaneous coupling through different channels. For the minimization of  $J_{\text{TV}}$  we use a heuristic scheme as in [25], by alternating iterations for the minimization of  $J$  and for the minimization of  $(|Fu^2|_{\text{TV}} + |Fu^3|_{\text{TV}})$ , compare also [19]. The corresponding results are shown in Figure 4 where the effect of the coupling (for the cases  $q = 2, \infty$ ) is further enhanced. The right picture in the second row of Figure 5 shows the result of the reconstruction in this latter case. The edges are perfectly recovered.

These numerical experiments confirm that the use of the joint sparsity measure  $\Phi^{(q)}$  associated to the curvelet representation can improve significantly the quality of the reconstructed color image. Better results are achieved by choosing  $q = \infty$  and by the adaptive choice of weights as indicators of the sparsity pattern. Further improvements can be achieved by channelwise edge enhancing, e.g., via total variation minimization. An application to the real case of the art frescoes is illustrated in Figure 6.

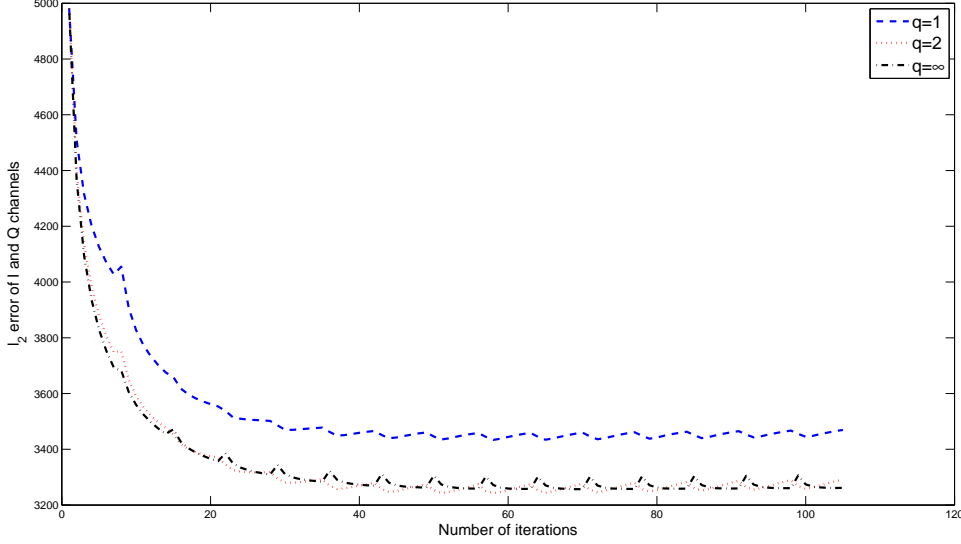


Figure 4: The  $\ell_2$  error between the *original color image* and the iterations of the algorithm is shown for different values of  $q = 1, 2, \infty$ . We have considered  $L_n = 7$  and  $n_{\max} = 15$ , the numbers of inner and outer iterations respectively. We have fixed here  $\omega_\lambda = 1/20$ ,  $\theta_\lambda = 10$ , and  $\rho_\lambda = 20 \times 2^{-j}$ . Further iterations of TV minimization are added in the outer loop to enforce edge enhancing.

## 7 Final Remarks

1. If the index set  $\Lambda$  is infinite then  $T^*T$  is represented as a biinfinite matrix and thus its evaluation might not be exactly numerically implementable. In a subsequent work we will consider the case  $\#\Lambda = \infty$  and the treatment of sparse (approximate) evaluations of biinfinite matrices in order to realize fast and convergent schemes also in this situation, compare also [38, 14, 15].

2. To exploit the optimal performance of the scheme, an extensive campaign of numerical experiments should be conducted in order to further refine the choice of parameters. It is also crucial to investigate the deeper relations among the parameter  $\rho_\lambda$ , the *multifractal analysis* as, e.g., in [30], and morphological image analysis. In particular, the parallel between the functional  $J$  and the  $\Gamma$ -approximation of the Mumford-Shah functional by Ambrosio and Tortorelli [1, 5] is suggestive:

$$F_\varepsilon(u, v) := \underbrace{\int_{\Omega} (u - g)^2 dx}_{\sim \mathcal{T}(u)} + \underbrace{\int_{\Omega} v^2 f(\nabla u) dx}_{\sim \sum_{\lambda} v_{\lambda} \|u\|_q} + \underbrace{\int_{\Omega} \varepsilon |\nabla u|^2 dx}_{\sim \sum_{\lambda} \omega_{\lambda} \|u\|_2^2} + \underbrace{\int_{\Omega} \left( \varepsilon |\nabla v|^2 + \frac{1}{4\varepsilon} (1 - v)^2 \right) dx}_{\sim \sum_{\lambda} \theta_{\lambda} (\rho_{\lambda} - v_{\lambda})^2},$$

where  $f$  is a suitable polyconvex function, e.g.,  $f(\nabla u) = (|\nabla u|^2 + |u_x \times u_y|) = (|\nabla u|^2 + |\text{adj}_2(\nabla u)|)$ ,  $\text{adj}_2(A)$  is the matrix of all  $2 \times 2$  minors of  $A$ . The minimization of this term enforces that derivatives of different channels are large only in the same directions.

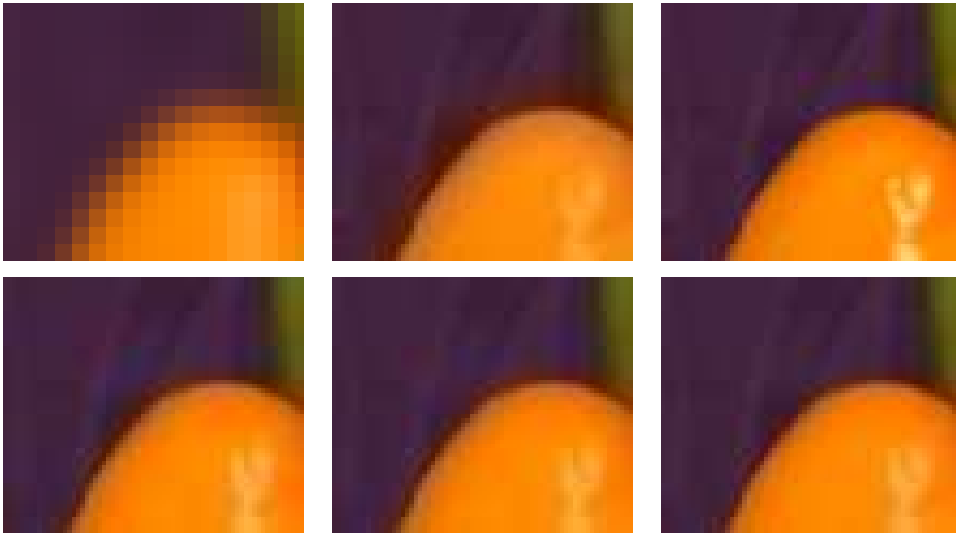


Figure 5: **First row.** *Left:* Portion of the low resolution color image. *Center:* Portion of the reconstructed color image by Gaussian interpolation and substitution of the  $Y$  channel with the gray level datum. Evident color artifacts appear at edges. *Right:* Portion of the original color image. **Second row.** *Left:* Portion of the reconstructed color image for  $q = 1$ ,  $L_n = 105$ , and  $n_{\max} = 1$ . *Center:* Portion of the reconstructed color image for  $q = \infty$ ,  $L_n = 7$ , and  $n_{\max} = 15$ . *Right:* Portion of the reconstructed color image for  $q = \infty$ ,  $L_n = 7$ ,  $n_{\max} = 15$ , and TV minimization.

According to the specific choices of  $\rho_\lambda$  to indicate the discontinuity set of  $u$ , and for  $\omega_\lambda = \varepsilon$  and  $\theta_\lambda = \frac{1}{4\varepsilon}$ , we may investigate the behavior of the functional  $J$  for  $\varepsilon \rightarrow 0$  and its relation with the Mumford-Shah functional. The term  $\sum_\lambda \frac{1}{4\varepsilon} (\rho_\lambda - v_\lambda)^2$  essentially counts the number of curvelets that, from a certain scale  $j$  on such that  $2^{-j} \sim \varepsilon$ , do overlap with the discontinuity set and are nearly tangent to the singularity. We conjecture that for  $\varepsilon \rightarrow 0$  and for a rectifiable curved discontinuity, this term estimates the length of the discontinuity.

3. While we were finishing this paper, we have been informed by G. Teschke of the results in [19]. In this manuscript the authors consider linear inverse problems where the solution is assumed to fulfill some general 1-homogeneous convex constraint. They develop an algorithm that amounts to a projected Landweber iteration and that provides an iterative approach to the solution of this inverse problem. In particular for the case  $\omega = (\omega_\lambda)_\lambda = 0$ , some of our results stated in Section 4 can be reformulated in this more general setting and therefore derived from [19]. However, for  $\omega \neq 0$  the sparsity measure  $\Psi_{v,\omega}^{(q)}$  as in (26) is not 1-homogeneous and the elaborations in Section 4 are needed. Moreover, for the relevant cases  $q = 1, 2, \infty$ , we express explicitly the projection  $P_{v/2}^{q'}$ . Due to their generality, the results in [19] do not provide concrete recipes to compute such projections.



Figure 6: *Left:* Low quality color image of the fresco dated to 1940. *Center:* High quality gray image of the fresco dated to 1920. Some details are not visible in the color version. *Right:* The reconstructed image after 6 outer iterations with 7 inner iterations each, for  $q = \infty$ . The final  $Y$  channel is substituted with the high resolution gray level datum. The discontinuities are enhanced and no artifact colors appear.

## 8 Conclusion

We have investigated joint sparsity measures with respect to frame expansions of vector valued functions. These sparsity measures generalize approaches valid for scalar functions and take into account common sparsity patterns through different channels. We have analyzed linear inverse problems with joint sparsity regularization as well as their efficient numerical solution by means of a novel algorithm based on thresholded Landweber iterations. We have provided the convergence analysis for a wide range of parameters. The role of the joint sparsity measure is twofold: to tighten the characterization of solutions of interest and to extract significant morphological properties which are a common feature of all the channels. By numerical applications in color image restoration, we have shown that joint sparsity significantly outperforms uncoupled constraints. We have presented the results of an application to a relevant real-world problem in art restoration. The wide range of applicability of our approach includes several other problems with coupled vector valued solutions, e.g., neuroimaging and distributed compressed sensing.

## References

- [1] L. Ambrosio and V. M. Tortorelli, *Approximation of functionals depending on jumps by elliptic functionals via  $\Gamma$ -convergence.*, Commun. Pure Appl. Math. **43** (1990), no. 8, 999–1036.
- [2] S. Anthoine, *Different Wavelet-based Approaches for the Separation of Noisy and Blurred Mixtures of Components. Application to Astrophysical Data.*, Ph.D. thesis, Princeton University, 2005.

- [3] D. Baron, M.B. Wakin, M.F. Duarte, S. Sarvotham, and R.G. Baraniuk, *Distributed Compressed Sensing*, preprint (2005).
- [4] S. Boyd and L. Vandenberghe, *Convex Optimization.*, Cambridge University Press, 2004.
- [5] A. Brook, R. Kimmel, and N.A. Sochen, *Variational restoration and edge detection for color images.*, J. Math. Imaging Vis. **18** (2003), no. 3, 247–268.
- [6] E. Candes, J. Romberg, and T. Tao, *Exact signal reconstruction from highly incomplete frequency information*, IEEE Trans. Inf. Theory **52** (2006), no. 2, 489–509.
- [7] E. Candes and T. Tao, *Near Optimal Signal Recovery From Random Projections And Universal Encoding Strategies*, IEEE Trans. Inf. Theory (to appear).
- [8] E. J. Candès, L. Demanet, D. L. Donoho, and L. Ying, *Fast Discrete Curvelet Transforms*, (2005).
- [9] E. J. Candès and D. L. Donoho, *New tight frames of curvelets and optimal representations of objects with piecewise  $C^2$  singularities.*, Commun. Pure Appl. Math. **57** (2004), no. 2, 219–266.
- [10] C. Canuto and K. Urban, *Adaptive optimization of convex functionals in Banach spaces*, SIAM J. Numer. Anal. **42** (2004), no. 5, 2043–2075.
- [11] O. Christensen, *An Introduction to Frames and Riesz Bases*, Birkhäuser, Boston, 2003 (english).
- [12] A. Cohen, *Numerical Analysis of Wavelet Methods.*, Studies in Mathematics and its Applications 32. Amsterdam: North-Holland., 2003.
- [13] A. Cohen, M. Hoffmann, and M. Reiss, *Adaptive wavelet Galerkin methods for linear inverse problems.*, SIAM J. Numer. Anal. **42** (2004), no. 4, 1479–1501.
- [14] S. Dahlke, M. Fornasier, and T. Raasch, *Adaptive frame methods for elliptic operator equations*, Adv. Comput. Math. (2006), to appear.
- [15] S. Dahlke, M. Fornasier, T. Raasch, R. Stevenson, and M. Werner, *Adaptive frame methods for elliptic operator equations: The steepest descent approach*, preprint, 2005.
- [16] S. Dahlke and P. Maass, *An outline of adaptive wavelet Galerkin methods for Tikhonov regularization of inverse parabolic problems.*, Hon, Yiu-Chung (ed.) et al., Recent development in theories and numerics. Proceedings of the international conference on inverse problems, Hong Kong, China, January 9-12, 2002. River Edge, NJ: World Scientific. 56-66 , 2003.
- [17] I. Daubechies, M. Defrise, and C. De Mol, *An iterative thresholding algorithm for linear inverse problems*, Comm. Pure Appl. Math. **57** (2004), no. 11, 1413–1457.

- [18] I. Daubechies and G. Teschke, *Variational image restoration by means of wavelets: Simultaneous decomposition, deblurring, and denoising.*, Appl. Comput. Harmon. Anal. **19** (2005), no. 1, 1–16.
- [19] I. Daubechies, G. Teschke, and L. Vese, *Iteratively solving linear inverse problems under general convex constraints*, preprint, 2006.
- [20] D. L. Donoho, *Superresolution via sparsity constraints.*, SIAM J. Math. Anal. **23** (1992), no. 5, 1309–1331.
- [21] ———, *De-noising by soft-thresholding.*, IEEE Trans. Inf. Theory **41** (1995), no. 3, 613–627.
- [22] ———, *Nonlinear solution of linear inverse problems by wavelet-vaguelette decomposition.*, Appl. Comput. Harmon. Anal. **2** (1995), no. 2, 101–126.
- [23] D.L. Donoho, *Compressed Sensing*, IEEE Trans. Inf. Theory **52** (2006), no. 4, 1289–1306.
- [24] I. Ekeland and R. Témam, *Convex analysis and variational problems*, SIAM, 1999.
- [25] M. Elad, J.-L. Starck, P. Querre, and D. L. Donoho, *Simultaneous cartoon and texture image inpainting using morphological component analysis (MCA)*, Appl. Comput. Harmon. Anal. **19** (2005), 340–358.
- [26] H. W. Engl, M. Hanke, and A. Neubauer, *Regularization of inverse problems.*, Mathematics and its Applications (Dordrecht). 375. Dordrecht: Kluwer Academic Publishers., 1996.
- [27] M. Fornasier and D. Toniolo, *Computer-based recomposition of the frescoes in the Ovetari Chapel in the Church of the Eremitani in Padua. Methodology and initial results, (English/Italian)*, in “Mantegna nella chiesa degli Eremitani a Padova. Il recupero possibile”, Ed. Skira, 2003.
- [28] ———, *Fast, robust, and efficient 2D pattern recognition for re-assembling fragmented digital images*, Pattern Recognition **38** (2005), 2074–2087.
- [29] A.C. Gilbert, M.J. Strauss, and J. Tropp, *Algorithms for simultaneous sparse approximation. Part I: Greedy pursuit*, Signal Processing **86** (2006), 572–588.
- [30] S. Jaffard, *Beyond Besov spaces. I: Distributions of wavelet coefficients.*, J. Fourier Anal. Appl. **10** (2004), no. 3, 221–246.
- [31] ———, *Beyond Besov spaces. II: Oscillation spaces.*, Constructive Approximation **21** (2005), no. 1, 29–61.
- [32] S. Kunis and H. Rauhut, *Random sampling of sparse trigonometric polynomials II - Orthogonal Matching Pursuit versus Basis Pursuit*, preprint (2006).
- [33] S. Mallat, *A Wavelet Tour of Signal Processing. 2nd Ed.*, San Diego, CA: Academic Press., 1999.

- [34] D. Mumford and J. Shah, *Optimal approximations by piecewise smooth functions and associated variational problems.*, Commun. Pure Appl. Math. **42** (1989), no. 5, 577–685.
- [35] R. Ramlau and G. Teschke, *Tikhonov replacement functionals for iteratively solving nonlinear operator equations.*, Inverse Probl. **21** (2005), no. 5, 1571–1592.
- [36] H. Rauhut, *Random sampling of sparse trigonometric polynomials*, Appl. Comput. Harm. Anal. (to appear).
- [37] R.T. Rockafellar and R.J.B. Wets, *Variational analysis*, Grundlehren der Mathematischen Wissenschaften, vol. 317, Springer-Verlag, Berlin, 1998.
- [38] R. Stevenson, *Adaptive solution of operator equations using wavelet frames*, SIAM J. Numer. Anal **41** (2003), no. 3, 1074–1100.
- [39] G. Teschke, *Multi-frames in thresholding iterations for nonlinear operator equations with mixed sparsity constraints*, preprint, 2005.
- [40] J. Tropp, *Algorithms for simultaneous sparse approximation. Part II: Convex relaxation*, Signal Processing **86** (2006), 589–602.



# SAMPLE FILE FOR SIAM L<sup>A</sup>T<sub>E</sub>X MACRO PACKAGE\*

PAUL DUGGAN<sup>†</sup> AND VARIOUS A. U. THORS<sup>‡</sup>

**Abstract.** An example of SIAM L<sup>A</sup>T<sub>E</sub>X macros is presented. Various aspects of composing manuscripts for SIAM's journal series are illustrated with actual examples from accepted manuscripts. SIAM's stylistic standards are adhered to throughout, and illustrated.

**Key words.** sign-nonsingular matrix, LU-factorization, indicator polynomial

**AMS subject classifications.** 15A15, 15A09, 15A23

**1. Introduction and examples.** This paper presents a sample file for the use of SIAM's L<sup>A</sup>T<sub>E</sub>X macro package. It illustrates the features of the macro package, using actual examples culled from various papers published in SIAM's journals. It is to be expected that this sample will provide examples of how to use the macros to generate standard elements of journal papers, e.g., theorems, definitions, or figures. This paper also serves as an example of SIAM's stylistic preferences for the formatting of such elements as bibliographic references, displayed equations, and equation arrays, among others. Some special circumstances are not dealt with in this sample file; for such information one should see the included documentation file.

*Note:* This paper is not to be read in any form for content. The conglomeration of equations, lemmas, and other text elements were put together solely for typographic illustrative purposes and don't make any sense as lemmas, equations, etc.

**1.1. Sample text.** Let  $S = [s_{ij}]$  ( $1 \leq i, j \leq n$ ) be a  $(0, 1, -1)$ -matrix of order  $n$ . Then  $S$  is a *sign-nonsingular matrix* (SNS-matrix) provided that each real matrix with the same sign pattern as  $S$  is nonsingular. There has been considerable recent interest in constructing and characterizing SNS-matrices [1], [4]. There has also been interest in strong forms of sign-nonsingularity [2]. In this paper we give a new generalization of SNS-matrices and investigate some of their basic properties.

Let  $S = [s_{ij}]$  be a  $(0, 1, -1)$ -matrix of order  $n$  and let  $C = [c_{ij}]$  be a real matrix of order  $n$ . The pair  $(S, C)$  is called a *matrix pair of order  $n$* . Throughout,  $X = [x_{ij}]$  denotes a matrix of order  $n$  whose entries are algebraically independent indeterminates over the real field. Let  $S \circ X$  denote the Hadamard product (entrywise product) of  $S$  and  $X$ . We say that the pair  $(S, C)$  is a *sign-nonsingular matrix pair of order  $n$* , abbreviated *SNS-matrix pair of order  $n$* , provided that the matrix

$$A = S \circ X + C$$

is nonsingular for all positive real values of the  $x_{ij}$ . If  $C = O$  then the pair  $(S, O)$  is a SNS-matrix pair if and only if  $S$  is a SNS-matrix. If  $S = O$  then the pair  $(O, C)$  is a SNS-matrix pair if and only if  $C$  is nonsingular. Thus SNS-matrix pairs include both nonsingular matrices and sign-nonsingular matrices as special cases.

The pairs  $(S, C)$  with

$$S = \begin{bmatrix} 1 & 0 \\ 0 & 0 \end{bmatrix}, \quad C = \begin{bmatrix} 1 & 1 \\ 1 & 1 \end{bmatrix}$$

---

\*This work was supported by the Society for Industrial and Applied Mathematics, Philadelphia, Pennsylvania.

<sup>†</sup>Composition Department, Society for Industrial and Applied Mathematics, 3600 Univeristy City Science Center, Philadelphia, Pennsylvania, 19104-2688 ([duggan@siam.org](mailto:duggan@siam.org)).

<sup>‡</sup>Various Affiliations, supported by various foundation grants.

and

$$S = \begin{bmatrix} 1 & 1 & 0 \\ 1 & 1 & 0 \\ 0 & 0 & 0 \end{bmatrix}, \quad C = \begin{bmatrix} 0 & 0 & 1 \\ 0 & 2 & 0 \\ 3 & 0 & 0 \end{bmatrix}$$

are examples of SNS-matrix pairs.

**1.2. A remuneration list.** In this paper we consider the evaluation of integrals of the following forms:

$$(1.1) \quad \int_a^b \left( \sum_i E_i B_{i,k,x}(t) \right) \left( \sum_j F_j B_{j,l,y}(t) \right) dt,$$

$$(1.2) \quad \int_a^b f(t) \left( \sum_i E_i B_{i,k,x}(t) \right) dt,$$

where  $B_{i,k,x}$  is the  $i$ th B-spline of order  $k$  defined over the knots  $x_i, x_{i+1}, \dots, x_{i+k}$ . We will consider B-splines normalized so that their integral is one. The splines may be of different orders and defined on different knot sequences  $x$  and  $y$ . Often the limits of integration will be the entire real line,  $-\infty$  to  $+\infty$ . Note that (1.1) is a special case of (1.2) where  $f(t)$  is a spline.

There are five different methods for calculating (1.1) that will be considered:

1. Use Gauss quadrature on each interval.
2. Convert the integral to a linear combination of integrals of products of B-splines and provide a recurrence for integrating the product of a pair of B-splines.
3. Convert the sums of B-splines to piecewise Bézier format and integrate segment by segment using the properties of the Bernstein polynomials.
4. Express the product of a pair of B-splines as a linear combination of B-splines. Use this to reformulate the integrand as a linear combination of B-splines, and integrate term by term.
5. Integrate by parts.

Of these five, only methods 1 and 5 are suitable for calculating (1.2). The first four methods will be touched on and the last will be discussed at length.

**1.3. Some displayed equations and  $\{\text{eqnarray}\}$ s.** By introducing the product topology on  $R^{m \times m} \times R^{n \times n}$  with the induced inner product

$$(1.3) \quad \langle (A_1, B_1), (A_2, B_2) \rangle := \langle A_1, A_2 \rangle + \langle B_1, B_2 \rangle,$$

we calculate the Fréchet derivative of  $F$  as follows:

$$(1.4) \quad \begin{aligned} F'(U, V)(H, K) &= \langle R(U, V), H\Sigma V^T + U\Sigma K^T - P(H\Sigma V^T + U\Sigma K^T) \rangle \\ &= \langle R(U, V), H\Sigma V^T + U\Sigma K^T \rangle \\ &= \langle R(U, V)V\Sigma^T, H \rangle + \langle \Sigma^T U^T R(U, V), K^T \rangle. \end{aligned}$$

In the middle line of (1.4) we have used the fact that the range of  $R$  is always perpendicular to the range of  $P$ . The gradient  $\nabla F$  of  $F$ , therefore, may be interpreted as the pair of matrices:

$$(1.5) \quad \nabla F(U, V) = (R(U, V)V\Sigma^T, R(U, V)^T U\Sigma) \in R^{m \times m} \times R^{n \times n}.$$

Because of the product topology, we know

$$(1.6) \quad \mathcal{T}_{(U,V)}(\mathcal{O}(m) \times \mathcal{O}(n)) = \mathcal{T}_U \mathcal{O}(m) \times \mathcal{T}_V \mathcal{O}(n),$$

where  $\mathcal{T}_{(U,V)}(\mathcal{O}(m) \times \mathcal{O}(n))$  stands for the tangent space to the manifold  $\mathcal{O}(m) \times \mathcal{O}(n)$  at  $(U, V) \in \mathcal{O}(m) \times \mathcal{O}(n)$  and so on. The projection of  $\nabla F(U, V)$  onto  $\mathcal{T}_{(U,V)}(\mathcal{O}(m) \times \mathcal{O}(n))$ , therefore, is the product of the projection of the first component of  $\nabla F(U, V)$  onto  $\mathcal{T}_U \mathcal{O}(m)$  and the projection of the second component of  $\nabla F(U, V)$  onto  $\mathcal{T}_V \mathcal{O}(n)$ . In particular, we claim that the projection  $g(U, V)$  of the gradient  $\nabla F(U, V)$  onto  $\mathcal{T}_{(U,V)}(\mathcal{O}(m) \times \mathcal{O}(n))$  is given by the pair of matrices:

$$(1.7) \quad g(U, V) = \left( \frac{R(U, V)V\Sigma^T U^T - U\Sigma V^T R(U, V)^T}{2} U, \right. \\ \left. \frac{R(U, V)^T U\Sigma V^T - V\Sigma^T U^T R(U, V)}{2} V \right).$$

Thus, the vector field

$$(1.8) \quad \frac{d(U, V)}{dt} = -g(U, V)$$

defines a steepest descent flow on the manifold  $\mathcal{O}(m) \times \mathcal{O}(n)$  for the objective function  $F(U, V)$ .

**2. Main results.** Let  $(S, C)$  be a matrix pair of order  $n$ . The determinant

$$\det(S \circ X + C)$$

is a polynomial in the indeterminates of  $X$  of degree at most  $n$  over the real field. We call this polynomial the *indicator polynomial* of the matrix pair  $(S, C)$  because of the following proposition.

**THEOREM 2.1.** *The matrix pair  $(S, C)$  is a SNS-matrix pair if and only if all the nonzero coefficients in its indicator polynomial have the same sign and there is at least one nonzero coefficient.*

*Proof.* Assume that  $(S, C)$  is a SNS-matrix pair. Clearly the indicator polynomial has a nonzero coefficient. Consider a monomial

$$(2.1) \quad b_{i_1, \dots, i_k; j_1, \dots, j_k} x_{i_1 j_1} \cdots x_{i_k j_k}$$

occurring in the indicator polynomial with a nonzero coefficient. By taking the  $x_{ij}$  that occur in (2.1) large and all others small, we see that any monomial that occurs in the indicator polynomial with a nonzero coefficient can be made to dominate all others. Hence all the nonzero coefficients have the same sign. The converse is immediate.  $\square$

For SNS-matrix pairs  $(S, C)$  with  $C = O$  the indicator polynomial is a homogeneous polynomial of degree  $n$ . In this case Theorem 2.1 is a standard fact about SNS-matrices.

**LEMMA 2.2 (Stability).** *Given  $T > 0$ , suppose that  $\|\epsilon(t)\|_{1,2} \leq h^{q-2}$  for  $0 \leq t \leq T$  and  $q \geq 6$ . Then there exists a positive number  $B$  that depends on  $T$  and the exact solution  $\psi$  only such that for all  $0 \leq t \leq T$ ,*

$$(2.2) \quad \frac{d}{dt} \|\epsilon(t)\|_{1,2} \leq B(h^{q-3/2} + \|\epsilon(t)\|_{1,2}).$$

The function  $B(T)$  can be chosen to be nondecreasing in time.

**THEOREM 2.3.** *The maximum number of nonzero entries in a SNS-matrix  $S$  of order  $n$  equals*

$$\frac{n^2 + 3n - 2}{2}$$

with equality if and only if there exist permutation matrices such that  $P|S|Q = T_n$  where

$$(2.3) \quad T_n = \begin{bmatrix} 1 & 1 & \cdots & 1 & 1 & 1 \\ 1 & 1 & \cdots & 1 & 1 & 1 \\ 0 & 1 & \cdots & 1 & 1 & 1 \\ \vdots & \vdots & \ddots & \vdots & \vdots & \vdots \\ 0 & 0 & \cdots & 1 & 1 & 1 \\ 0 & 0 & \cdots & 0 & 1 & 1 \end{bmatrix}.$$

We note for later use that each submatrix of  $T_n$  of order  $n - 1$  has all 1s on its main diagonal.

We now obtain a bound on the number of nonzero entries of  $S$  in a SNS-matrix pair  $(S, C)$  in terms of the degree of the indicator polynomial. We denote the strictly upper triangular  $(0,1)$ -matrix of order  $m$  with all 1s above the main diagonal by  $U_m$ . The all 1s matrix of size  $m$  by  $p$  is denoted by  $J_{m,p}$ .

**PROPOSITION 2.4** (Convolution theorem). *Let*

$$a * u(t) = \int_0^t a(t - \tau)u(\tau)d\tau, \quad t \in (0, \infty).$$

Then

$$\widehat{a * u}(s) = \widehat{a}(s)\widehat{u}(s).$$

**LEMMA 2.5.** *For  $s_0 > 0$ , if*

$$\int_0^\infty e^{-2s_0 t} v^{(1)}(t)v(t)dt \leq 0,$$

then

$$\int_0^\infty e^{-2s_0 t} v^2(t)dt \leq \frac{1}{2s_0} v^2(0).$$

*Proof.* Applying integration by parts, we obtain

$$\begin{aligned} \int_0^\infty e^{-2s_0 t} [v^2(t) - v^2(0)]dt &= \lim_{t \rightarrow \infty} \left( -\frac{1}{2s_0} e^{-2s_0 t} v^2(t) \right) + \frac{1}{s_0} \int_0^\infty e^{-2s_0 t} v^{(1)}(t)v(t)dt \\ &\leq \frac{1}{s_0} \int_0^\infty e^{-2s_0 t} v^{(1)}(t)v(t)dt \leq 0. \end{aligned}$$

Thus

$$\int_0^\infty e^{-2s_0 t} v^2(t)dt \leq v^2(0) \int_0^\infty e^{-2s_0 t} dt = \frac{1}{2s_0} v^2(0). \quad \square$$

COROLLARY 2.6. Let  $\mathbf{E}$  satisfy (5)–(6) and suppose  $\mathbf{E}^h$  satisfies (7) and (8) with a general  $\mathbf{G}$ . Let  $\mathbf{G} = \nabla \times \Phi + \nabla p$ ,  $p \in H_0^1(\Omega)$ . Suppose that  $\nabla p$  and  $\nabla \times \Phi$  satisfy all the assumptions of Theorems 4.1 and 4.2, respectively. In addition suppose all the regularity assumptions of Theorems 4.1–4.2 are satisfied. Then for  $0 \leq t \leq T$  and  $0 < \epsilon \leq \epsilon_0$  there exists a constant  $C = C(\epsilon, T)$  such that

$$\|(\mathbf{E} - \mathbf{E}^h)(t)\|_0 \leq Ch^{k+1-\epsilon},$$

where  $C$  also depends on the constants given in Theorems 4.1 and 4.2.

DEFINITION 2.7. Let  $S$  be an isolated invariant set with isolating neighborhood  $N$ . An index pair for  $S$  is a pair of compact sets  $(N_1, N_0)$  with  $N_0 \subset N_1 \subset N$  such that:

- (i)  $cl(N_1 \setminus N_0)$  is an isolating neighborhood for  $S$ .
- (ii)  $N_i$  is positively invariant relative to  $N$  for  $i = 0, 1$ , i.e., given  $x \in N_i$  and  $x \cdot [0, t] \subset N$ , then  $x \cdot [0, t] \subset N_i$ .
- (iii)  $N_0$  is an exit set for  $N_1$ , i.e. if  $x \in N_1$ ,  $x \cdot [0, \infty) \not\subset N_1$ , then there is a  $T \geq 0$  such that  $x \cdot [0, T] \subset N_1$  and  $x \cdot T \in N_0$ .

**2.1. Numerical experiments.** We conducted numerical experiments in computing inexact Newton steps for discretizations of a *modified Bratu problem*, given by

$$(2.4) \quad \begin{aligned} \Delta w + ce^w + d \frac{\partial w}{\partial x} &= f \quad \text{in } D, \\ w &= 0 \quad \text{on } \partial D, \end{aligned}$$

where  $c$  and  $d$  are constants. The actual Bratu problem has  $d = 0$  and  $f \equiv 0$ . It provides a simplified model of nonlinear diffusion phenomena, e.g., in combustion and semiconductors, and has been considered by Glowinski, Keller, and Rheinhardt [11], as well as by a number of other investigators; see [11] and the references therein. See also problem 3 by Glowinski and Keller and problem 7 by Mittelmann in the collection of nonlinear model problems assembled by Moré [13]. The modified problem (2.4) has been used as a test problem for inexact Newton methods by Brown and Saad [7].

In our experiments, we took  $D = [0, 1] \times [0, 1]$ ,  $f \equiv 0$ ,  $c = d = 10$ , and discretized (2.4) using the usual second-order centered differences over a  $100 \times 100$  mesh of equally spaced points in  $D$ . In GMRES( $m$ ), we took  $m = 10$  and used fast Poisson right preconditioning as in the experiments in §2. The computing environment was as described in §2. All computing was done in double precision.

In the first set of experiments, we allowed each method to run for 40 GMRES( $m$ ) iterations, starting with zero as the initial approximate solution, after which the limit of residual norm reduction had been reached. The results are shown in Fig. 2.1. In Fig. 2.1, the top curve was produced by method FD1. The second curve from the top is actually a superposition of the curves produced by methods EHA2 and FD2; the two curves are visually indistinguishable. Similarly, the third curve from the top is a superposition of the curves produced by methods EHA4 and FD4, and the fourth curve from the top, which lies barely above the bottom curve, is a superposition of the curves produced by methods EHA6 and FD6. The bottom curve was produced by method A.

In the second set of experiments, our purpose was to assess the relative amount of computational work required by the methods which use higher-order differencing to reach comparable levels of residual norm reduction. We compared pairs of methods

FIG. 2.1.  $\log_{10}$  of the residual norm versus the number of GMRES( $m$ ) iterations for the finite difference methods.

TABLE 2.1

Statistics over 20 trials of GMRES( $m$ ) iteration numbers,  $F$ -evaluations, and run times required to reduce the residual norm by a factor of  $\epsilon$ . For each method, the number of GMRES( $m$ ) iterations and  $F$ -evaluations was the same in every trial.

Method	$\epsilon$	Number of Iterations	Number of $F$ -Evaluations	Mean Run Time (Seconds)	Standard Deviation
EHA2	$10^{-10}$	26	32	47.12	.1048
FD2	$10^{-10}$	26	58	53.79	.1829
EHA4	$10^{-12}$	30	42	56.76	.1855
FD4	$10^{-12}$	30	132	81.35	.3730
EHA6	$10^{-12}$	30	48	58.56	.1952
FD6	$10^{-12}$	30	198	100.6	.3278

EHA2 and FD2, EHA4 and FD4, and EHA6 and FD6 by observing in each of 20 trials the number of GMRES( $m$ ) iterations, number of  $F$ -evaluations, and run time required by each method to reduce the residual norm by a factor of  $\epsilon$ , where for each pair of methods  $\epsilon$  was chosen to be somewhat greater than the limiting ratio of final to initial residual norms obtainable by the methods. In these trials, the initial approximate solutions were obtained by generating random components as in the similar experiments in §2. We note that for every method, the numbers of GMRES( $m$ ) iterations and  $F$ -evaluations required before termination did not vary at all over the 20 trials. The GMRES( $m$ ) iteration counts, numbers of  $F$ -evaluations, and means and standard deviations of the run times are given in Table 2.1.

In our first set of experiments, we took  $c = d = 10$  and used right preconditioning with a fast Poisson solver from FISHPACK [16], which is very effective for these fairly small values of  $c$  and  $d$ . We first started each method with zero as the initial approximate solution and allowed it to run for 40 GMRES( $m$ ) iterations, after which the limit of residual norm reduction had been reached. Figure 2.2 shows plots of the logarithm of the Euclidean norm of the residual versus the number of GMRES( $m$ ) iterations for the three methods. We note that in Fig. 2.2 and in all other figures below, the plotted residual norms were not the values maintained by GMRES( $m$ ), but rather were computed as accurately as possible “from scratch.” That is, at each

FIG. 2.2.  $\log_{10}$  of the residual norm versus the number of GMRES( $m$ ) iterations for  $c = d = 10$  with fast Poisson preconditioning. Solid curve: Algorithm EHA; dotted curve: FDP method; dashed curve: FSP method.

GMRES( $m$ ) iteration, the current approximate solution was formed and its product with the coefficient matrix was subtracted from the right-hand side, all in double precision. It was important to compute the residual norms in this way because the values maintained by GMRES( $m$ ) become increasingly untrustworthy as the limits of residual norm reduction are neared; see [17]. It is seen in Fig. 2.2 that Algorithm EHA achieved the same ultimate level of residual norm reduction as the FDP method and required only a few more GMRES( $m$ ) iterations to do so.

In our second set of experiments, we took  $c = d = 100$  and carried out trials analogous to those in the first set above. No preconditioning was used in these experiments, both because we wanted to compare the methods without preconditioning and because the fast Poisson preconditioning used in the first set of experiments is not cost effective for these large values of  $c$  and  $d$ . We first allowed each method to run for 600 GMRES( $m$ ) iterations, starting with zero as the initial approximate solution, after which the limit of residual norm reduction had been reached.

**Acknowledgments.** The author thanks the anonymous authors whose work largely constitutes this sample file. He also thanks the INFO-TeX mailing list for the valuable indirect assistance he received.

#### REFERENCES

- [1] R. A. BRUALDI AND B. L. SHADER, *On sign-nonsingular matrices and the conversion of the permanent into the determinant*, in Applied Geometry and Discrete Mathematics, The Victor Klee Festschrift, P. Gritzmann and B. Sturmfels, eds., American Mathematical Society, Providence, RI, 1991, pp. 117–134.
- [2] J. DREW, C. R. JOHNSON, AND P. VAN DEN DRIESSCHE, *Strong forms of nonsingularity*, Linear Algebra Appl., 162 (1992), to appear.
- [3] P. M. GIBSON, *Conversion of the permanent into the determinant*, Proc. Amer. Math. Soc., 27 (1971), pp. 471–476.

- [4] V. KLEE, R. LADNER, AND R. MANBER, *Signsolvability revisited*, Linear Algebra Appl., 59 (1984), pp. 131–157.
- [5] K. MUROTA, *LU-decomposition of a matrix with entries of different kinds*, Linear Algebra Appl., 49 (1983), pp. 275–283.
- [6] O. AXELSSON, *Conjugate gradient type methods for unsymmetric and inconsistent systems of linear equations*, Linear Algebra Appl., 29 (1980), pp. 1–16.
- [7] P. N. BROWN AND Y. SAAD, *Hybrid Krylov methods for nonlinear systems of equations*, SIAM J. Sci. Statist. Comput., 11 (1990), pp. 450–481.
- [8] R. S. DEMBO, S. C. EISENSTAT, AND T. STEIHAUG, *Inexact Newton methods*, SIAM J. Numer. Anal., 19 (1982), pp. 400–408.
- [9] S. C. EISENSTAT, H. C. ELMAN, AND M. H. SCHULTZ, *Variational iterative methods for nonsymmetric systems of linear equations*, SIAM J. Numer. Anal., 20 (1983), pp. 345–357.
- [10] H. C. ELMAN, *Iterative methods for large, sparse, nonsymmetric systems of linear equations*, Ph.D. thesis, Department of Computer Science, Yale University, New Haven, CT, 1982.
- [11] R. GLOWINSKI, H. B. KELLER, AND L. RHEINHART, *Continuation-conjugate gradient methods for the least-squares solution of nonlinear boundary value problems*, SIAM J. Sci. Statist. Comput., 6 (1985), pp. 793–832.
- [12] G. H. GOLUB AND C. F. VAN LOAN, *Matrix Computations*, Second ed., The Johns Hopkins University Press, Baltimore, MD, 1989.
- [13] J. J. MORÉ, *A collection of nonlinear model problems*, in Computational Solutions of Nonlinear Systems of Equations, E. L. Allgower and K. Georg, eds., Lectures in Applied Mathematics, Vol. 26, American Mathematical Society, Providence, RI, 1990, pp. 723–762.
- [14] Y. SAAD, *Krylov subspace methods for solving large unsymmetric linear systems*, Math. Comp., 37 (1981), pp. 105–126.
- [15] Y. SAAD AND M. H. SCHULTZ, *GMRES: A generalized minimal residual method for solving nonsymmetric linear systems*, SIAM J. Sci. Statist. Comput., 7 (1986), pp. 856–869.
- [16] P. N. SWARZTRAUBER AND R. A. SWEET, *Efficient FORTRAN subprograms for the solution of elliptic partial differential equations*, ACM Trans. Math. Software, 5 (1979), pp. 352–364.
- [17] H. F. WALKER, *Implementation of the GMRES method using Householder transformations*, SIAM J. Sci. Statist. Comput., 9 (1988), pp. 152–163.
- [18] ———, *Implementations of the GMRES method*, Computer Phys. Comm., 53 (1989), pp. 311–320.